

Hesselø Offshore Wind Farm

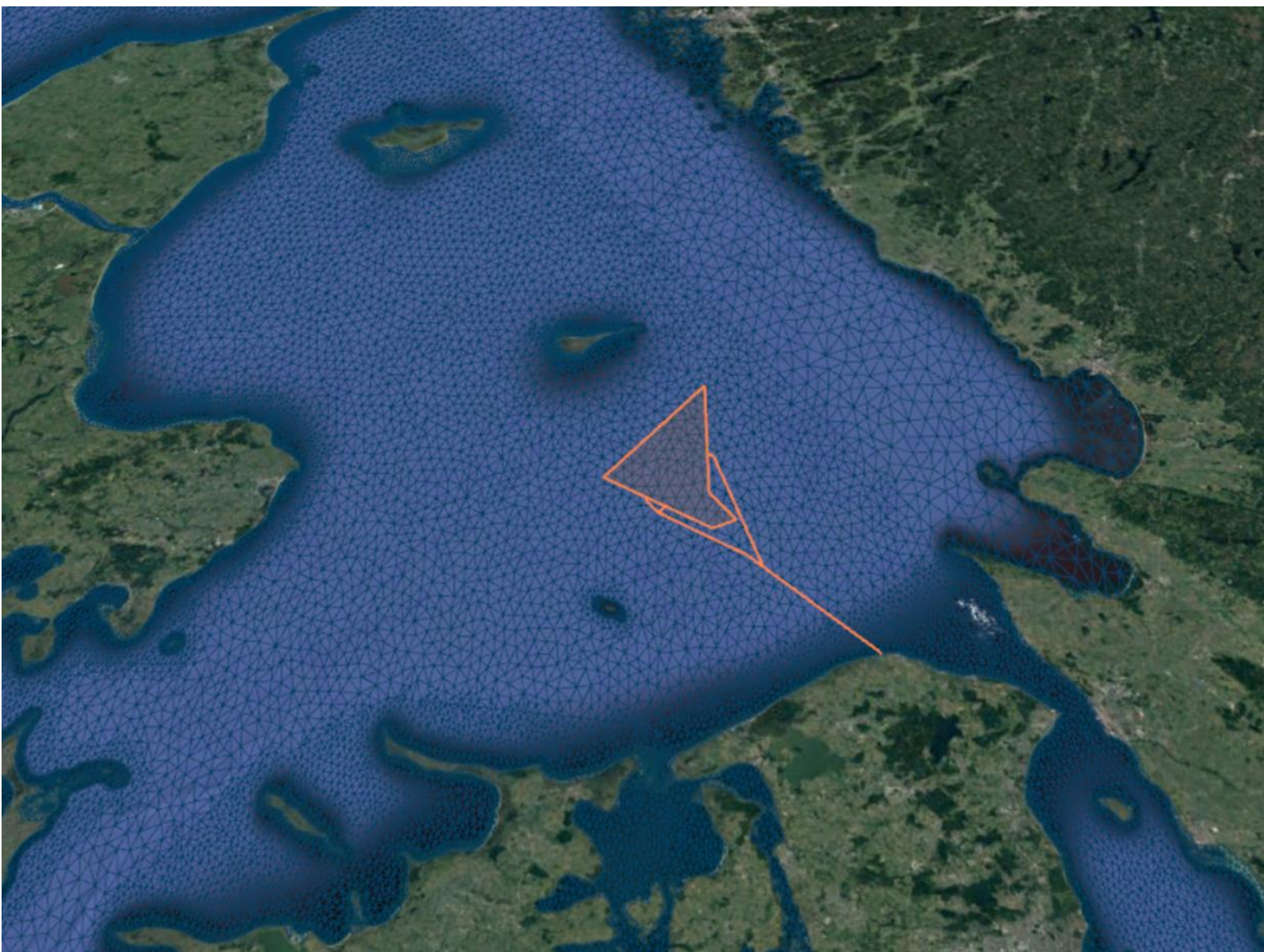
Weather Windows Analysis

Technical Report

24 March 2022

ENERGINET

Prepared for Energinet Eltransmission A/S





Hesselø Offshore Wind Farm

Weather Windows Analysis

Prepared for: Energinet Eltransmission A/S
Represented by Mr Kim Parsberg Jakobsen

Project Manager: Matthew Easton
Quality Supervisor: Matthew Easton
Author: Simone de Lemos
Project No.: 11826722
Approved by: Jesper Fuchs
Approval date: 24 March 2022
Revision: Final 1.0
Classification: **Open**
File name: 11826722_ENDK_Hesselø_WeatherWindow_RPT.docx

Contents

Executive Summary	1
1 Introduction	2
1.1 Background to the project.....	2
1.2 Aims and objectives.....	2
1.3 Layout of this report.....	3
2 Selection of Analysis Points	5
3 Study Data Basis	6
3.1 Atmospheric model (COSMO-REA6).....	6
3.2 Danish waters hydrodynamic model	10
3.3 Danish waters spectral wave model.....	16
4 General Metocean Conditions	19
4.1 Significant Wave Height (H_{m0}).....	19
4.2 Current speeds	21
4.3 Wind speeds at 10 mMSL	23
4.4 Water levels	25
5 Weather Window Methodology	26
5.1 Description of analysis methodology.....	26
5.2 Example of weather window results.....	27
6 Deliverables (Digital Appendix)	29
7 References	33

Figures

Figure 1.1	Map showing the location of the Hesselø OWF site	3
Figure 2.1	Map showing the four weather window analysis points.....	5
Figure 3.1	Numerical grid of the CREA6 model at the Hesselø OWF	7
Figure 3.2	Validation of CREA6 wind speeds at Anholt Havn	8
Figure 3.3	Validation of CREA6 wind speeds at Anholt Havn for 'open sea' directions only	9
Figure 3.4	Computational domain of DHI's Danish Waters hydrodynamic models (HD_{DKW}).....	11
Figure 3.5	Computational mesh and bathymetry of HD_{DKW} around the Hesselø OWF	11
Figure 3.6	Validation of HD_{DKW} residual water level at Hornbæk Havn	13
Figure 3.7	Histogram comparison depth-averaged current speed at Anholt OWF.....	14
Figure 3.8	Histogram comparison total depth-averaged current speed at Hesselø F-LiDAR	15
Figure 3.9	Computational mesh and bathymetry of SW_{DKW} around the Hesselø OWF	17
Figure 3.10	Validation of SW_{DKW} significant wave height at Anholt OWF	18
Figure 4.1	Annual variability of significant wave height at analysis point OWF-2.....	19
Figure 4.2	Seasonal wave rose plots at analysis point OWF-2	20
Figure 4.3	Annual variability of depth-averaged current speed at analysis point OWF-2	21
Figure 4.4	Seasonal total depth-averaged current speed roses at analysis point OWF-2.....	22
Figure 4.5	Annual variability of 10 mMSL wind speed at analysis point OWF-2	23
Figure 4.6	Seasonal 10 mMSL wind rose plots at analysis point OWF-2.....	24
Figure 4.7	Annual (all-year) probability distribution of total water levels at analysis point OWF-2	25
Figure 5.1	Example of weather-window analysis of H_{m0} at analysis point OWF-2	28
Figure 6.1	The digital appendix contains one folder per analysis point	29
Figure 6.2	Digital Appendix containing one folder per metocean parameter.....	30

Figure 6.3	Digital Appendix showing the definition of duration	30
Figure 6.4	Digital Appendix showing the thirteen (13) durations considered	31
Figure 6.5	Files containing the weather window analysis results	31
Figure 6.6	Example of weather wind results in Microsoft Excel format	32

Tables

Table 2.1	Summary of weather window analysis points	5
-----------	---	---

Appendices

Appendix A Definition of Model Quality Indices

Nomenclature

Abbreviations	
API	Application Programming Interface
CORDEX	Coordinated Regional Climate Downscaling Experiment
COSMO	COnsortium for Small-Scale MOdelling
CREA6	COSMO Reanalysis 6
DEA	Danish Energy Agency
DKW	Danish Waters
DMI	Danish Meteorological Institute
DWD	Deutscher Wetterdienst
ECMWF	European Centre for Medium-Range Weather Forecasts
EMODnet	European Marine Observation and Data Network
HD	Hydrodynamic
MSL	Mean Sea Level
MW	Megawatt
NWP	Numerical Weather Prediction
OWF	Offshore Wind Farm
RANS	Reynolds' Averaged Navier-Stokes
SMHI	Swedish Meteorological and Hydrological Institute
SW	Spectral Wave
UTM	Universal Transverse Mercator
WGS	World Geodetic System

Subscripts	
DKW	Danish Waters
NE	North Europe

Definitions	
Time	Times are relative to UTC
Levels	Levels are relative to mean sea level (MSL) or still water level (SWL) as specified
Directions	Wind: °N coming from and positive clockwise Waves: °N coming from and positive clockwise Current: °N going towards and positive clockwise

Symbols	
CS	Depth-averaged current speed
CD	Depth-averaged current direction
H_{m0}	Spectral significant wave height
MWD	Mean wave direction
WS_{10}	Wind speed at 10 m above MSL
WL	Water level

Executive Summary

The Hesselø offshore wind farm (OWF) is a project development located within Danish territorial waters, approximately 30 km north of Zealand and 20 km from the island of Hesselø in the Kattegat. This report and its accompanying appendices provide information on operational weather windows within the Hesselø OWF site and along its export cable corridor.

A weather window is defined as the continued occurrence of a given minimum interval (duration) during which the weather conditions (e.g., the wind speed or wave height) are below a certain critical threshold. Statistical information regarding the likelihood of weather windows is utilised for the planning of marine operations and for offshore construction activities.

Estimates of weather windows have been prepared at four locations: two locations within the Hesselø OWF site, and two locations on the export cable corridor. The analysis is based on long-term time-series data extracted from DHI's regional Danish Waters hindcast model database. This database contains information on the wind conditions, water levels, depth-averaged currents, and wave conditions with an output time interval of 1-hour over a continuous period of 24-years (1995 to 2018, inclusive). Details of the Danish Waters model database, its validation against local measurements, and the selected weather window analysis points are included in this report.

The general metocean conditions at the project site are described in term of the significant wave height (H_{m0}), water level (WL), depth-averaged current speed (CS), and the wind speed at 10 m above mean sea level (WS_{10}). Monthly statistics of weather windows are calculated for parameter specific threshold values for durations between 1 and 72-hours and certainty percentiles of 10%, 50%, and 90%. A summary of the methodology and an example of the analysis output are provided.

Due to the large amount of generated information, the complete set of weather window results at all four analysis points are provided as a digital appendix accompanying this report. This appendix takes the form of images and tables in Microsoft Excel file format. A guide explaining how the user should navigate through the digital appendix is included in this report.

1 Introduction

This document has been prepared for **Energinet Eltransmission A/S (Energinet)** by DHI A/S (DHI) in relation to weather windows analysis for the **Hesselø Offshore Wind Farm**.

1.1 Background to the project

The Energy Agreement of June 2018 sets out long-term energy policy for Denmark [1]. Among the aims of this agreement is to transform Denmark to a low carbon society that is independent of fossil fuels. Funding has been allocated to achieve a target of a 100% contribution of renewable energy to Denmark's electricity consumption by the year 2030. To achieve these targets, the energy agreement commits to the construction of three offshore wind farms. Each offshore wind farm (OWF) will have a capacity of at least 800 megawatts (MW).

In June 2020, the Danish Climate Agreement for Energy and Industry identified the Hesselø offshore wind farm as the second project to be developed under the Energy Agreement [2]. The wind farm is to be located within Hesselø Bugt, in the Kattegat, approximately 30 km north of Zealand and around 20 km from the island of Hesselø (Figure 1.1). The wind farm will have a total capacity of between 800 and 1,200 MW and cover an area of approximately 247 km². Power will be exported to land and connected to the electricity network at the Hovegård high-voltage electricity substation, west of the town of Ballerup. The wind farm must be completed by the end of 2027.

In July 2020, the Danish Energy Agency (DEA) instructed Energinet to initiate site investigations for the Hesselø OWF and to undertake supplementary studies and analyses. This includes the establishment of meteorological and oceanographic (metocean) data and documentation to support the tendering process and enable bidders to submit qualified economic bids.

1.2 Aims and objectives

The aim of the report is to provide an analysis of operational weather windows based on long-term hindcast metocean data at four locations within the Hesselø OWF and along its export cable corridor.

In the context of this study, a weather window is defined as the continued occurrence of a given minimum interval (duration) during which the weather conditions (e.g., the wind speed or wave height) are below a certain critical threshold. The weather window analysis provided herein has been performed for the following parameters and associated thresholds values:

- Significant wave height ($H_{m0} <$): 0.5 m to 5.0 m (at intervals of 0.5 m)
- Total water level ($WL <$): -2.0 m to +2.0 m (at intervals of 0.2 m)
- Total depth-averaged current speeds ($CS <$): 0.2 m/s to 1.0 m/s (at intervals of 0.2 m/s)
- Wind speed at 10 m above mean sea level ($WS_{10} <$): 5 m/s to 25 m/s (at intervals of 5 m/s)

For each parameter and threshold, the monthly statistics of weather window have been calculated for:

- Durations of 1, 6, 12, 18, 24, 30, 36, 42, 48, 54, 60, 66, and 72-hours
- Certainty percentiles (P) of 10%, 50%, and 90%

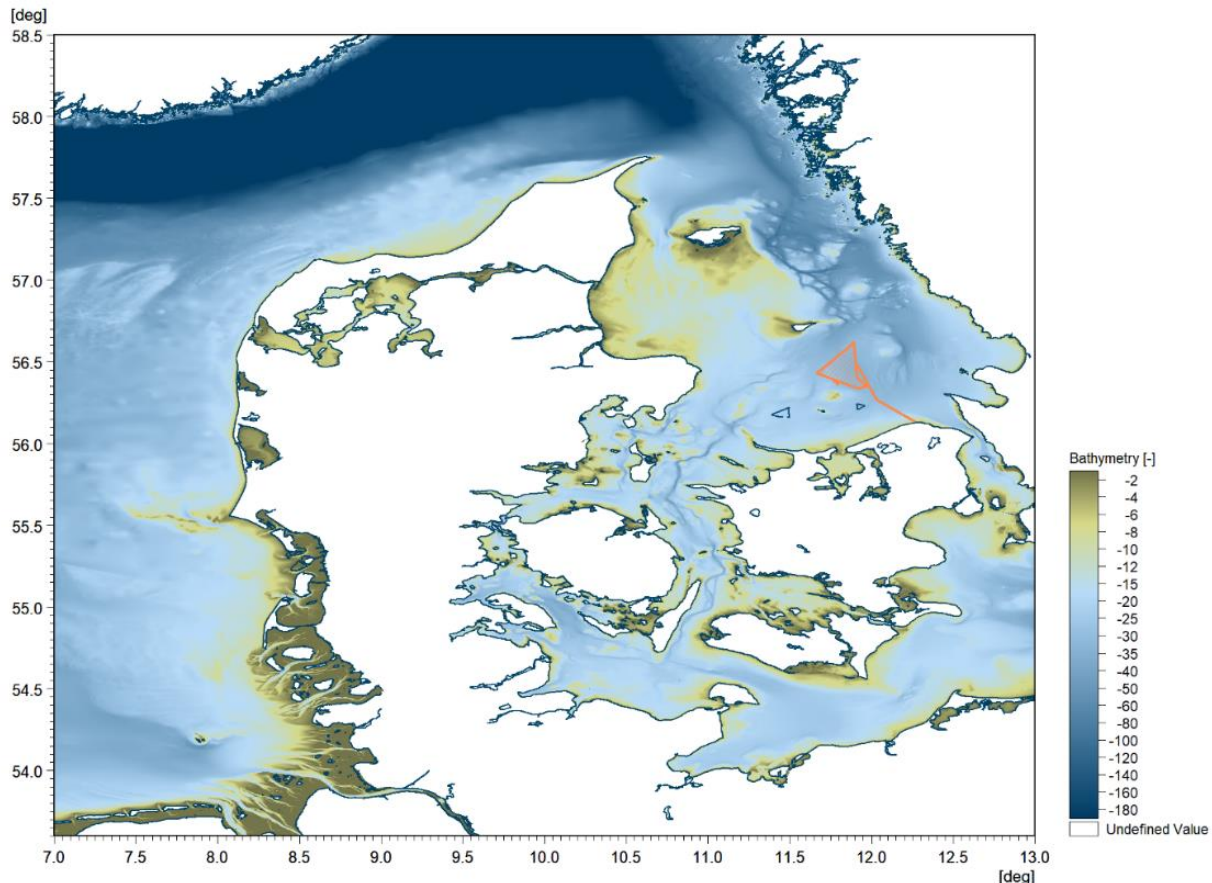


Figure 1.1 Map showing the location of the Hesselø OWF site
 The Hesselø OWF and its export cable corridor are shown by the orange polygon. The coloured shading shows the bathymetry in metres relative to lowest astronomical tide (LAT)

1.3 Layout of this report

The remaining sections of this report are organised as follows:

- [Section 2](#) describes the four analysis locations within the Hesselø OWF and export cable corridor at which the operational weather window analysis has been performed
- [Section 3](#) describes DHI's Danish Waters hindcast model database. This model database provided the long-term metocean data used as the input to the weather window analysis. The validation of the metocean models is also summarised
- [Section 4](#) provides a brief overview of the annual and seasonal variability of the metocean parameters at the Hesselø OWF site

- [Section 5](#) outlines the general methodology for the weather window analysis and provides an example of how the results should be interpreted
- [Section 6](#) provides a description of the digital appendix that is provided alongside this report. This section will guide the reader through the appendix which includes the full results of the weather window analyses at the Hesselø OWF and cable corridor

2 Selection of Analysis Points

This section describes the four analysis points within the Hesselø OWF and its export cable corridor at which the weather window analysis was performed.

The analysis points were chosen in collaboration with Energinet and were based on the bathymetric and metocean conditions across the project area. Table 2.1. summarises the names, coordinates, and seafloor elevation of the selected analysis points which are also shown on the map in Figure 2.1.

Analysis points OWF-1 and OWF-2 are located at the northern and south-eastern corner within the Hesselø OWF, respectively. Analysis points CC-1 and CC-2 are found along the export cable corridor, approximately 20 km and 5 km from the shoreline.

Table 2.1 Summary of weather window analysis points

The names, coordinates, and models depths at the four weather window analysis locations

Analysis point name	Longitude [°E]	Latitude [°N]	Seafloor elevation [mMSL]
OWF-1	11.882	56.590	-30.7
OWF-2	11.940	56.360	-31.3
CC-1	12.056	56.251	-28.3
CC-2	12.158	56.158	-13.9

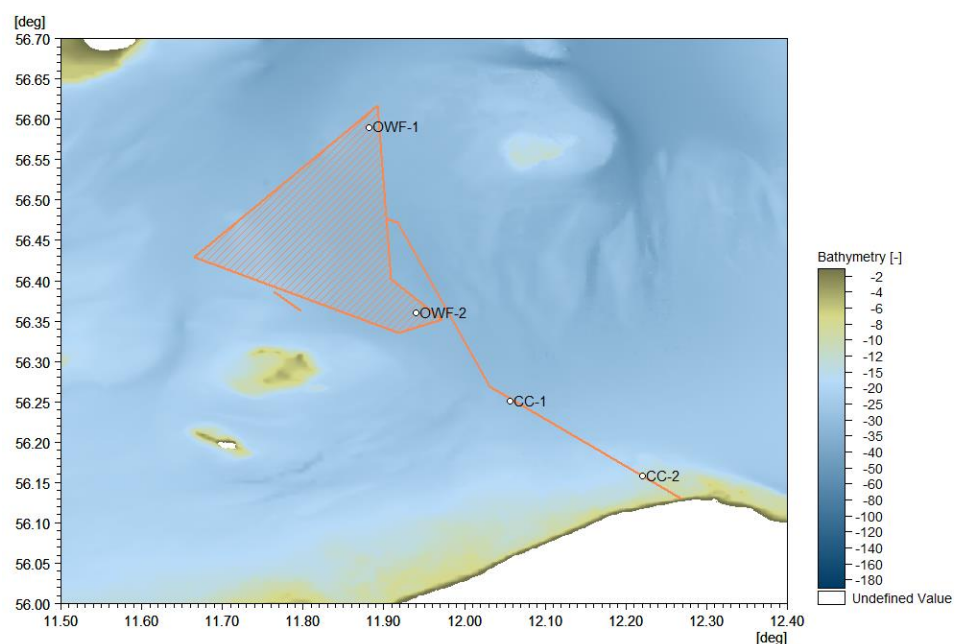


Figure 2.1 Map showing the four weather window analysis points

The Hesselø OWF and its export cable corridor are shown by the orange polygon. The coloured shading shows the bathymetry in metres relative to lowest astronomical tide (LAT)

3 Study Data Basis

The section describes DHI's Danish Waters hindcast model database. This database provided the long-term metocean time-series data that was used as input to the weather windows analysis at the Hesselø OWF.

DHI have established a regional hindcast model database of Danish Waters. The database provides a long-term repository of data to support marine projects and metocean studies in the seas around Denmark, including: the North Sea, Skagerrak, Kattegat, Northern Belt, Great Belt, Little Belt, Southern Belt, Øresund, and the Baltic Sea.

The hindcast model database spans a continuous period of 24-years (January 1995 to December 2018, inclusive) and consists of the following model components:

- Wind conditions from the COSMO-REA6 (**CREA6**) atmospheric model
- Water levels and depth-averaged currents from a two-dimensional hydrodynamic model, **HD_{DKW}**
- Ocean surface wave parameters from a spectral wave model, **SW_{DKW}**

The following sections provide a brief description of each of these models. For further detailed information, the reader is referred to the model setup, calibration, and validation report [3].

An overview of the validation of the model database against site measurements near the Hesselø project site are also included in the following sub-sections. The validation results are presented as time series, histogram, and scatter plots. [Appendix A](#) provides an overview of how the statistical measures (absolute and relative) are defined and some guidance on how they are to be interpreted. Additional validation of the models in the Kattegat can be found in the Hesselø OWF site metocean conditions assessment report [4].

3.1 Atmospheric model (COSMO-REA6)

The wind fields and atmospheric pressure for the Danish Waters model were adopted from the regional atmospheric reanalysis COSMO-REA6 (henceforth, CREA6). This model was developed by the Deutscher Wetterdienst (DWD) Hans-Ertel Centre for Weather Research at the University of Bonn¹ [5]. CREA6 employs the numerical weather prediction (NWP) model from the **CO**nsortium for **S**mall-**S**cale **MO**delling (**COSMO**)².

The model grid covers the EURO-CORDEX (European Coordinated Regional Climate Downscaling Experiment) EUR-11 domain, forced by the global reanalysis ERA-Interim from European Centre for Medium-Range Weather Forecasts (ECMWF)³ [6]. CREA6 provides wind and atmospheric pressure data every hour between 1995 and 2018. The atmospheric parameters of the

¹ <https://reanalysis.meteo.uni-bonn.de/?COSMO-REA6> – accessed March 2022

² [Consortium \(cosmo-model.org\)](https://www.cosmo-model.org/) – accessed March 2022

³ <https://www.ecmwf.int/en/forecasts/datasets/reanalysis-datasets/era-interim> - accessed March 2022

reanalysis are provided at a high-resolution of 0.055° , which is approximately $6.1 \text{ km latitude} \times 3.3 \text{ longitude}$ at the Hesselø OWF (Figure 3.1).

The following parameters were used for assessing the operational weather window in this study, with units in brackets

- Wind speed at 10 m above mean sea level [m/s]

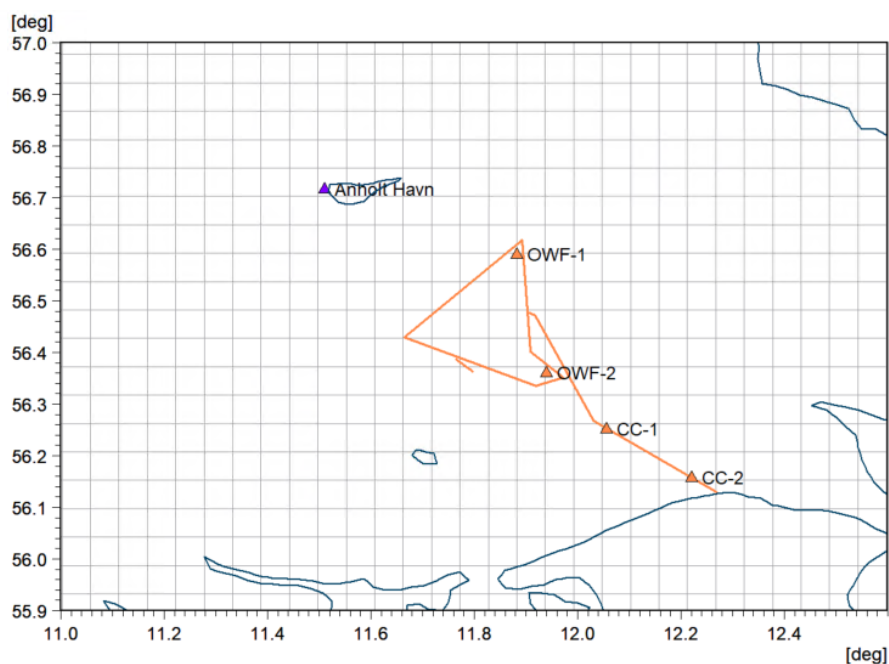


Figure 3.1 Numerical grid of the CREA6 model at the Hesselø OWF

The CREA6 model mesh is shown by the grey gridlines and the Hesselø OWF wind farm and export cable route are shown by the orange polygon. The weather window analysis points (OWF-1, OWF-2, CC-1, and CC-2) are shown by the orange triangle markers. The wind validation station at Anholt Havn is designated by the purple triangle

The CREA6 model was validated against wind speed data from the Anholt Havn measurement station, approximately 25 km northwest of the Hesselø OWF (see Figure 3.1). Time-series of wind speed were accessed via the Danish Meteorological Institute (DMI) Open Data Application Programming Interface (API)⁴. Please refer to Section 2.2.1 of [4] for more information on these measurement data.

The validation of 10 m modelled wind speed at the Anholt Havn is shown in Figure 3.2. The results show a very good replication of the measured wind speeds, with a small positive bias of $+0.04 \text{ m/s}$. However, there was a noticeably large scatter ($SI = 0.23$), particularly for measured wind speeds $< 12 \text{ m/s}$. The peak ratio ($PR = 1.0$) indicated that the largest wind speed events are very well captured by the CREA6 model (based on an average of 2 peak events per year).

⁴ [Danish Meteorological Institute - Open Data - DMI Open Data - Confluence \(govcloud.dk\)](https://open.data.dmi.dk/) – accessed March 2021

Figure 3.3 show the validation of 10 m wind speeds at Anholt Havn for ‘open sea’ directions only (i.e., the wind speeds associated with land directions from directional sectors centred at 60°N to 150°N have been removed). This results in a larger mean wind speed, a small negative bias (-0.36 m/s), a reduction in the scatter index (SI = 0.16), and a Q-Q fit line that is closer to the 1:1 line.

Please see Section 3.1 of [4] for further validation of CREA6 modelled wind speeds in the area around the Hesselø OWF.

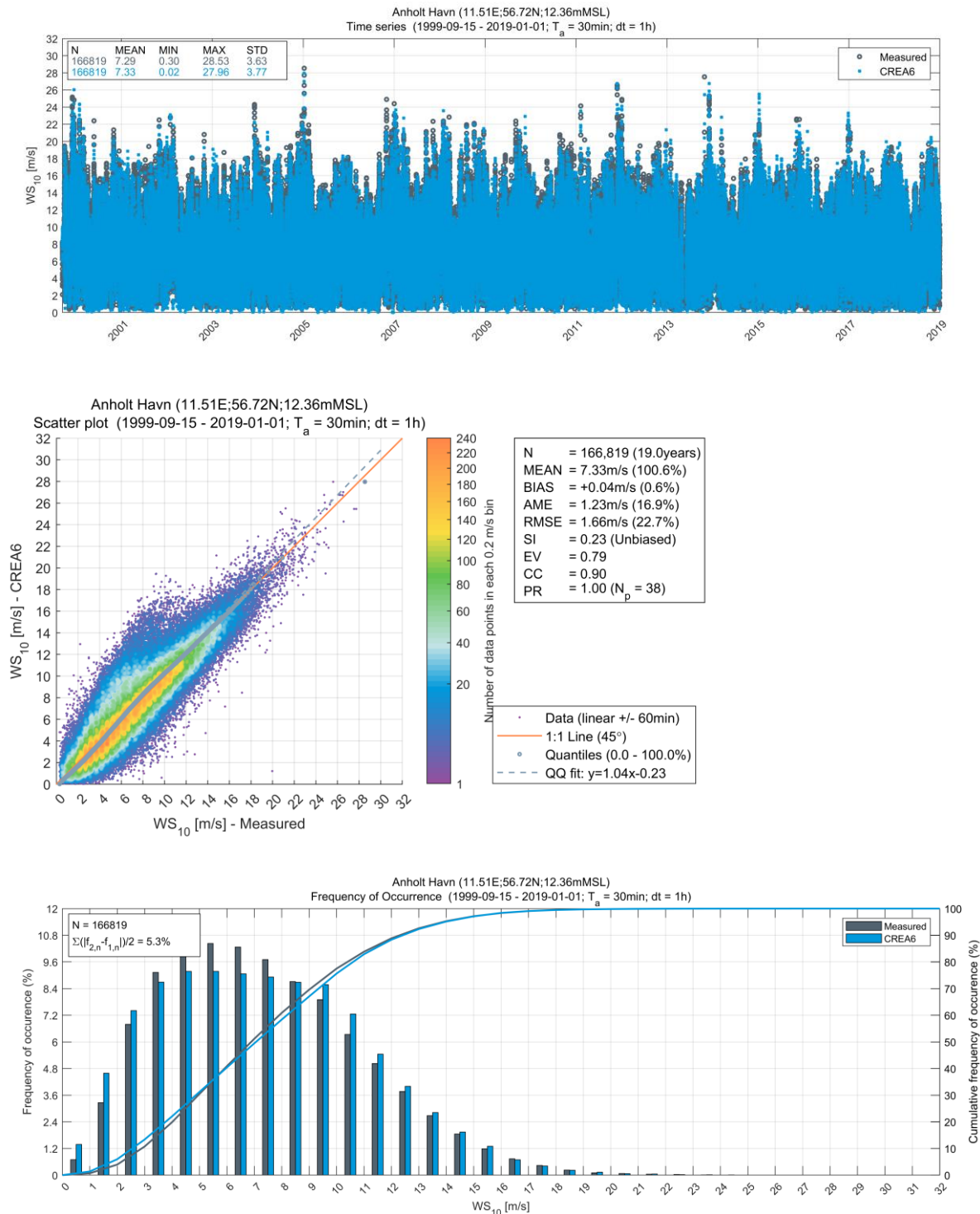


Figure 3.2 Validation of CREA6 wind speeds at Anholt Havn
 Time series (upper panel), scatter plot (central panel), and histogram (lower panel) comparison of modelled and measured residual water level

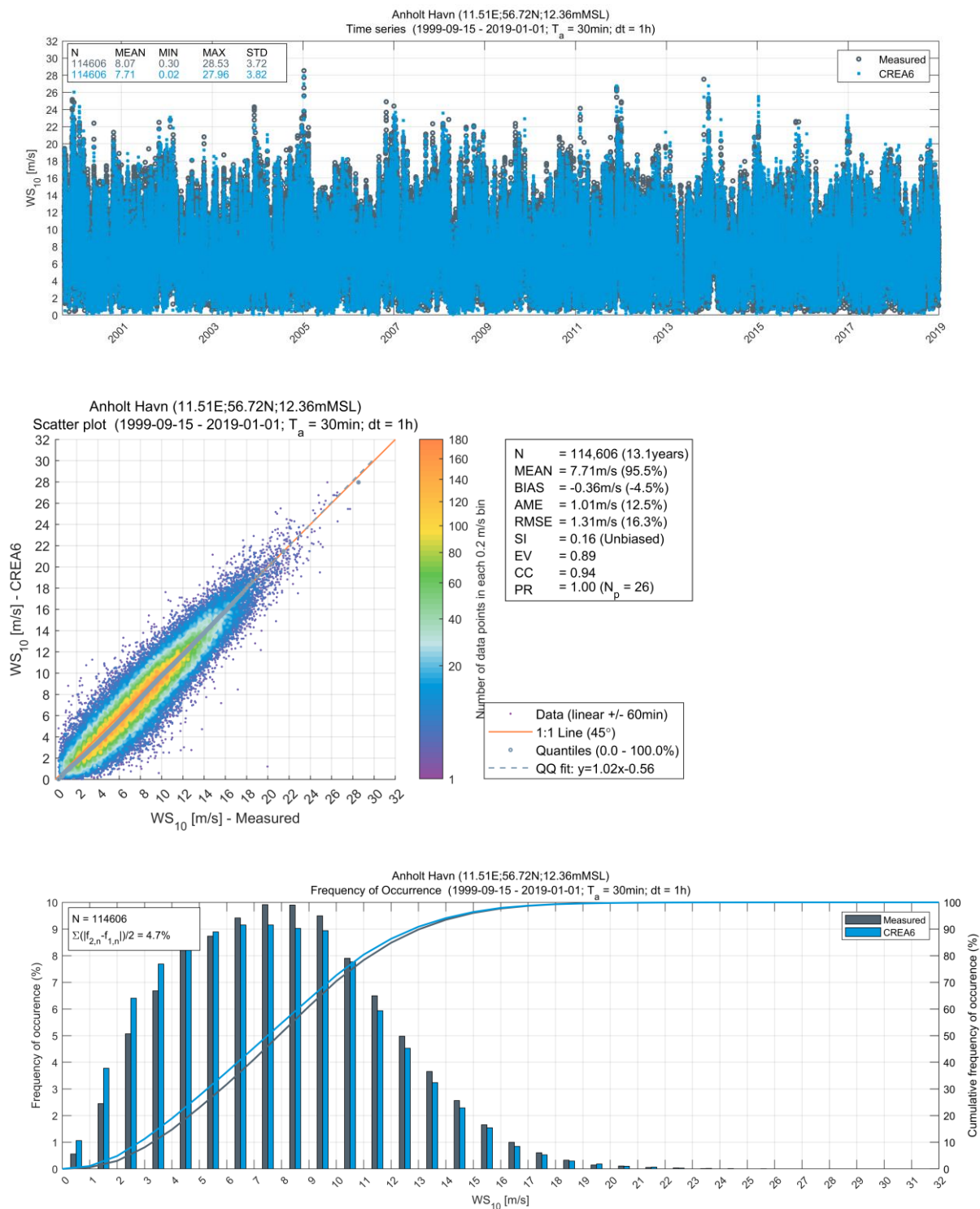


Figure 3.3 Validation of CREA6 wind speeds at Anholt Havn for ‘open sea’ directions only
Time series (upper panel), scatter plot (central panel), and histogram (lower panel) comparison of modelled and measured wind speed at 10 m. Wind speeds from directional sectors 60°N to 150°N are omitted from the comparison

3.2 Danish waters hydrodynamic model

DHI's Danish waters hydrodynamic model (**HD_{DKW}**) provides information on water levels and depth-averaged currents established through numerical modelling using the MIKE 21 Flow Model FM [7]. The model is based on the numerical solution of the 2D incompressible Reynolds-Averaged Navier-Stokes equations subject to the assumptions of Boussinesq and hydrostatic pressure. The model is applicable for the simulation of hydraulic and environmental phenomena in lakes, estuaries, bays, coastal areas, and seas, where stratification is negligible. The model can be used to simulate a wide range of hydraulic and related items, including tidal exchange, currents, and storm surges.

The HD_{DKW} model domain includes all Danish nearshore waters, plus areas offshore of Norway, Sweden, Poland, Germany, and the Netherlands (Figure 3.4). HD_{DKW} is based on an unstructured flexible mesh with refined resolution in shallow areas. The resolution of the model is 3 to 4 km in offshore areas, decreasing to around 2 km in Danish nearshore waters. Near to the Danish coastline, the resolution varies from 1 km to around 500 m. At the Hesselø offshore wind farm site, the resolution of the HD_{DKW} mesh is approximately 2 km (Figure 3.5).

The Danish waters hydrodynamic model is forced across its open (sea) boundaries by spatially and temporally varying water levels and depth-averaged currents extracted from DHI's regional North Europe Hydrodynamic model (HD_{NE}). HD_{DKW} also includes locally generated surge driven by the wind and air pressure fields from the CREA6 atmospheric model (see Section 3.1).

The outputs from HD_{DKW} include water level (WL) relative to mean-sea-level, depth-averaged current speed (CS), and depth-averaged current direction (CD), which are saved for each model mesh element at an output time interval of 0.5-hours.

The hydrodynamic setting of the Kattegat

The Hesselø OWF is located within the Kattegat, the major hydrographic transition zone between the brackish waters of the Baltic Sea (to the South) and the saline waters of the North Sea (to the North, via the Skagerrak). The waters of the Kattegat are generally described as two-layered consisting of:

- The northwards flow of the low salinity Baltic Current at the surface, with seasonally varying water salinity and temperature
- An underlying counter-current of oceanic waters from North Sea

The density gradients between the different water masses plays an important role in setting the circulation in the Kattegat. Strong wind-generated flows also modify the conditions over relatively short time periods. These three-dimensional phenomena will not be replicated by a two-dimensional hydrodynamic model such as HD_{DKW}, which is suited to describing barotropic flows where stratification is negligible.

If the currents and a possible stratification are critical for works within the Hesselø OWF and the cable corridor, an analysis of weather windows based on a three-dimensional hydrodynamic model should be considered.

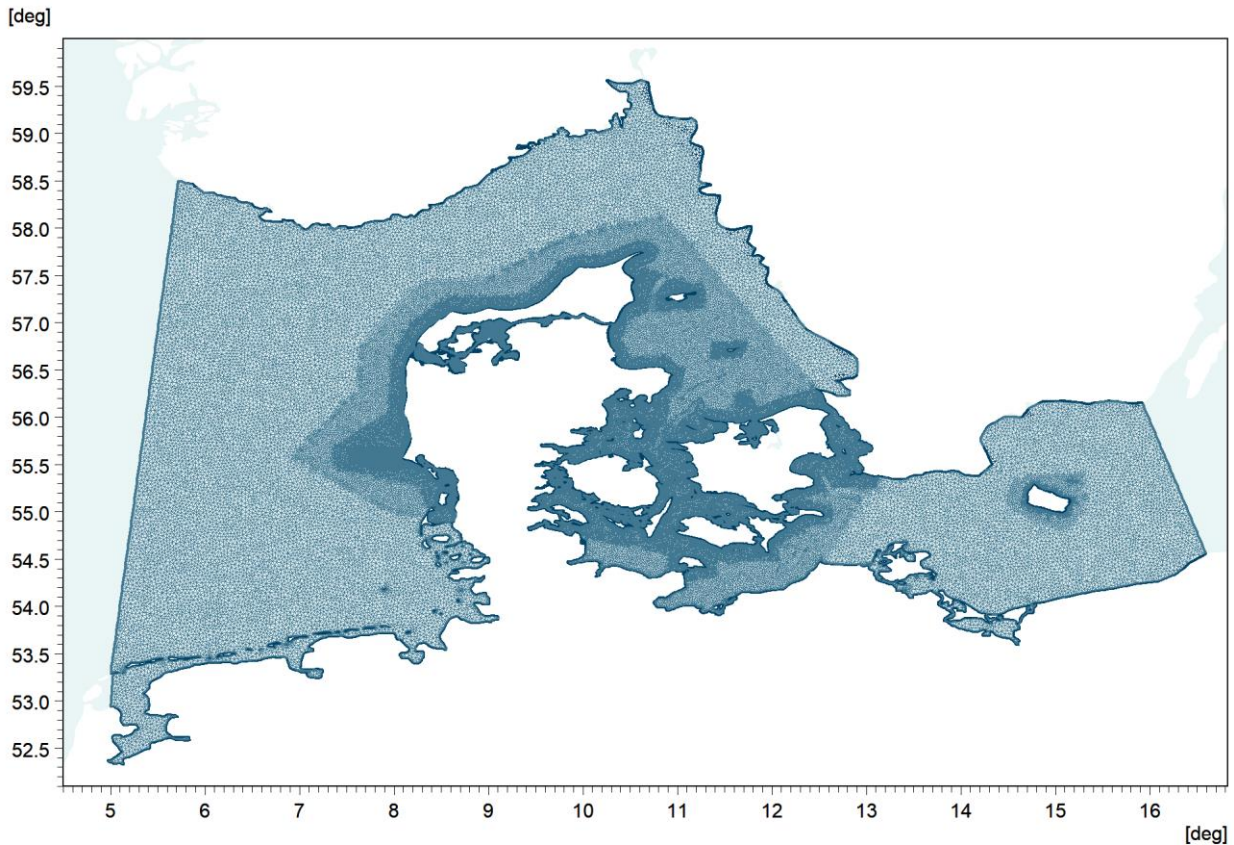


Figure 3.4 Computational domain of DHI's Danish Waters hydrodynamic models (HD_{DKW}). The hydrodynamic model mesh based on unstructured flexible elements, with refined resolution in shallow areas

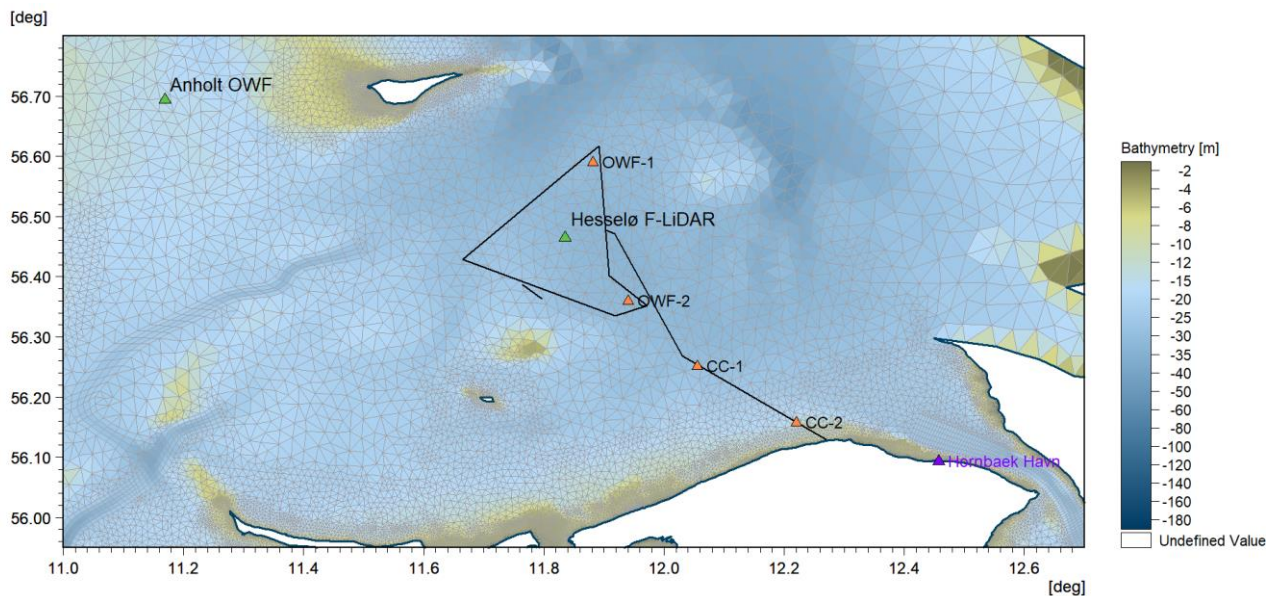


Figure 3.5 Computational mesh and bathymetry of HD_{DKW} around the Hesselø OWF. The unstructured flexible mesh is shown by the grey triangles and the Hesselø OWF development area and export cable corridor is designated by the black outline. The weather window analysis points (OWF-1, OWF-2, CC-1, and CC-2) are shown by the orange triangle markers. The water level validation station at Hornbæk Havn is designated by the purple triangle marker. The current validation stations at Anholt OWF and Hesselø F-LiDAR are shown by the green triangle markers

The HD_{DKW} model performance in terms of water levels was validated against measured data from Hornbæk Havn, which is the closest measurement station to the project site (see Figure 3.5). As the tidal variation in the area are very small, the validation was based on the non-tidal (i.e., residual/surge) component of the water level only. Both the modelled and measured water levels were subjected to a harmonic tidal analysis to separate the tidal and non-tidal components. The “de-tiding” was conducted using the U-tide package [8], a method which builds upon the tidal analysis approach defined by the Institute of Oceanographic Sciences (IOS) as described by [9]. Figure 3.6 shows a scatter plot validation result at Hornbæk Havn. The HD_{DKW} model provides a very good replication of the measured residual water levels at this station.

Please see Section 3.2.1 of [4] for additional water level validation of HD_{DKW} at other measurement stations around the Kattegat.

Validation of depth-averaged current speeds was performed at two stations: Anholt OWF and the Hesselø F-LiDAR (see Figure 3.5, and Section 2.2.3 of [4]). As explained previously (see [box on page 10](#)), the flow in the Kattegat is governed by three-dimensional flow phenomena and a two-dimensional model such as HD_{DKW} may not represent the current regime (or profile) accurately. The most informative means with which to validate the depth-averaged current speeds was to compare a distribution of modelled and measured values.

The upper panel of Figure 3.7 shows a histogram comparison of measured and HD_{DKW} modelled CS at Anholt OWF. The model overpredicts the frequency of the lower current speed (i.e., $CS \leq 0.15$ m/s) but underpredicts the frequency of higher current speeds (i.e., $CS > 0.15$ m/s). The lower panel of Figure 3.7 shows a histogram comparison of CS at Anholt OWF with a multiplication factor of 1.5 applied to the HD_{DKW} modelled values. The result is that the cumulative frequency of occurrence of CS more closely matches that of the measurements.

To verify this approach, Figure 3.8 shows a histogram comparison of depth-averaged current speeds at the Hesselø F-LiDAR. In this plot, the measured data are for the period 01 March to 27 September 2021, while the model results are based on the same date interval for the years 1995 to 2018. Mirroring the results at Anholt, the upper panel of Figure 3.8 shows that HD_{DKW} overpredicts the frequency of the lower current speed (i.e., $CS \leq 0.06$ m/s) while underpredicting the frequency of higher currents speeds (i.e., $CS \geq 0.08$ m/s). However, after applying a multiplication factor of 1.5 to the modelled values, the cumulative frequency of occurrence of CS more closely matches that of the measurements (lower panel of Figure 3.8).

The applied correction to the depth-averaged current speeds as described above is rather crude, and DHI consider that the current predictions from a two-dimensional model are not a suitable basis for a detailed assessment of the conditions at the Hesselø OWF. If the currents and a possible stratification are deemed critical for works within the Hesselø OWF and the cable corridor, it is the recommendation that further analyses are carried out using validated three-dimensional flow model data and/or long-term measurements of current profiles.

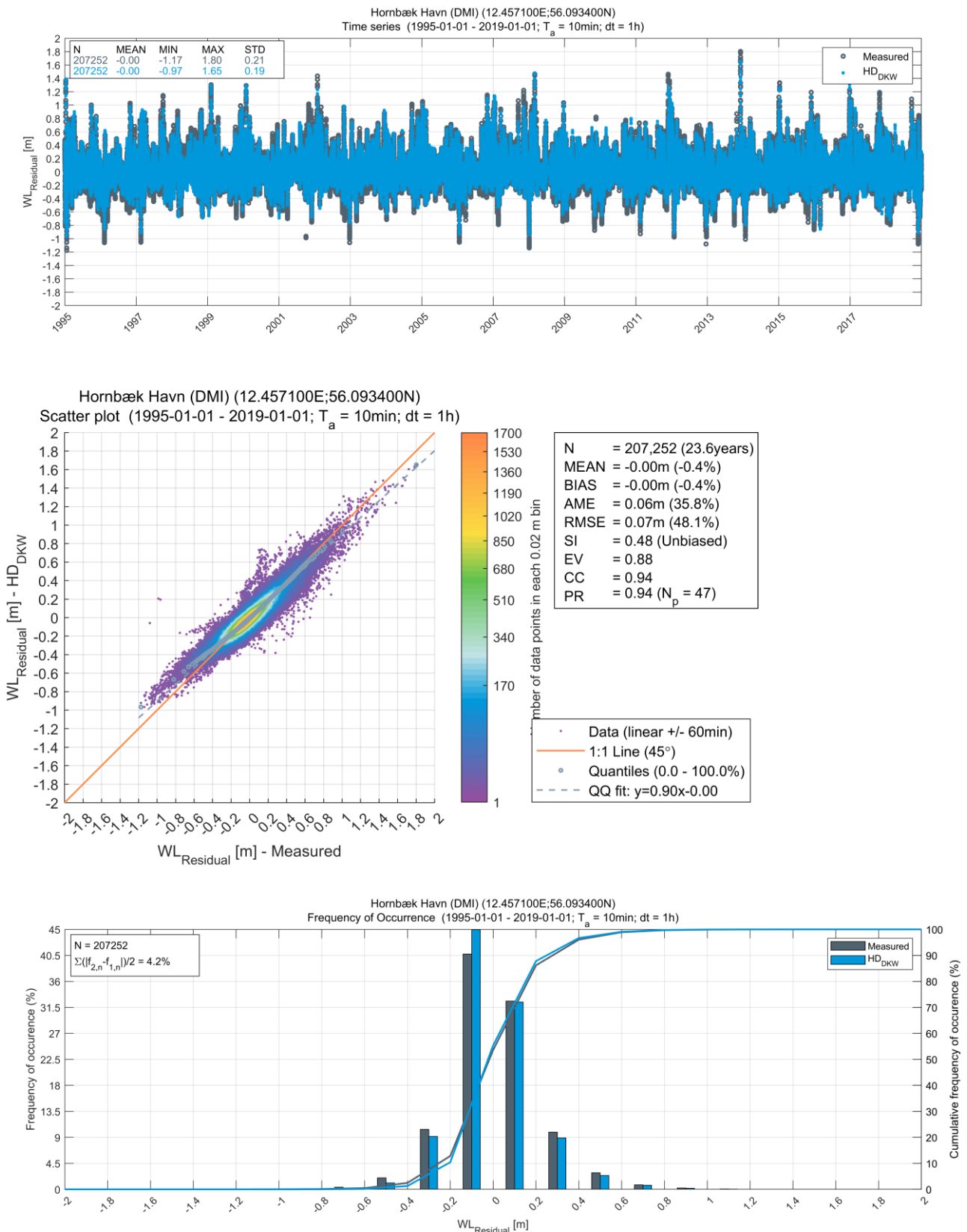


Figure 3.6 Validation of HD_{DKW} residual water level at Hornbæk Havn
Time series (upper panel), scatter plot (central panel), and histogram (lower panel) comparison of modelled and measured residual water level

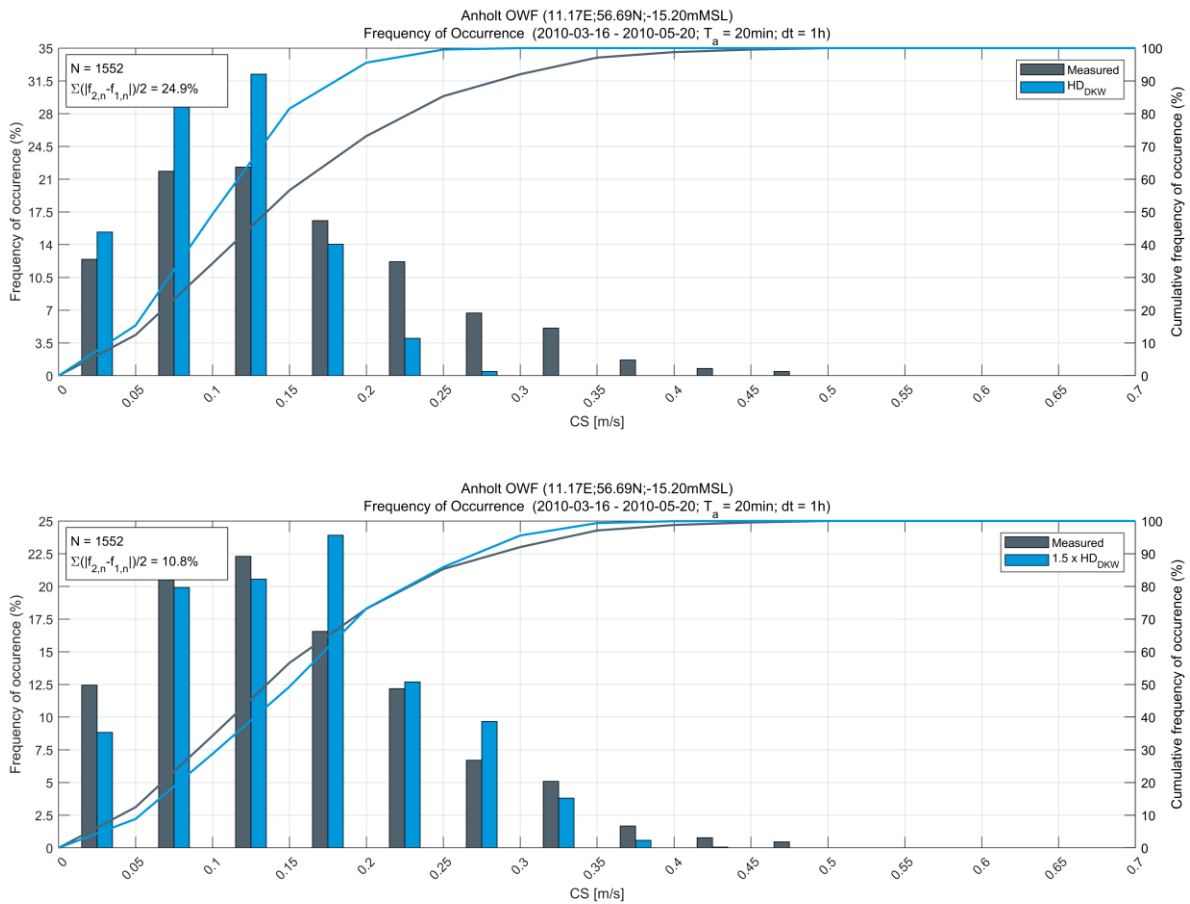


Figure 3.7 Histogram comparison depth-averaged current speed at Anholt OWF
 The comparison is based on the HD_{DKW} modelled depth-averaged current speeds (upper panel), and with a multiplication factor of 1.5 applied to the HD_{DKW} modelled depth-averaged current speeds plot (lower panel)

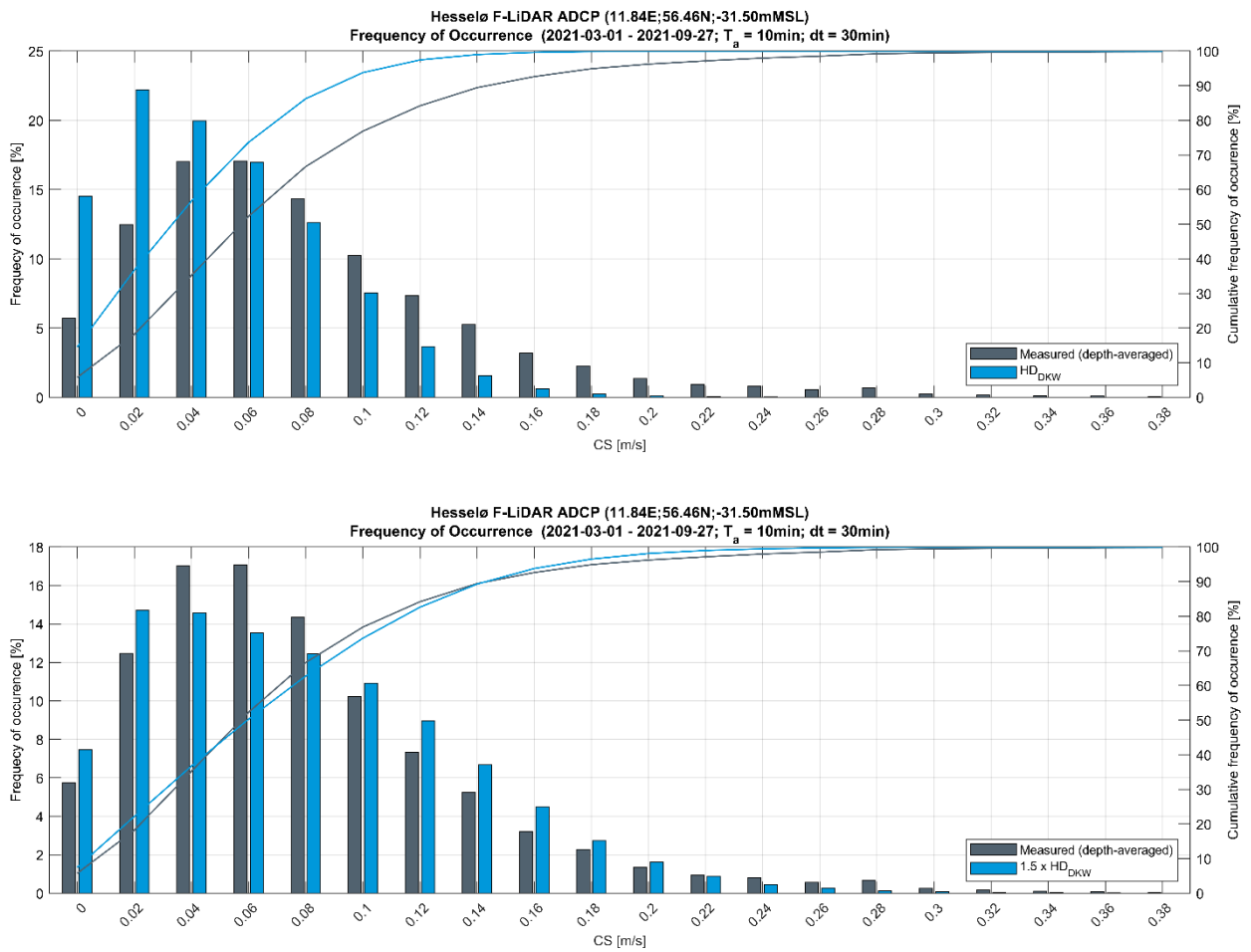


Figure 3.8 Histogram comparison total depth-averaged current speed at Hesselø F-LiDAR
 The measurements were recorded at the Hesselø between 01 March and 27 September 2021. The model values are calculated based on 24-years of HD_{DKW} depth-averaged current speeds between from 01 March and 27 September (1995 to 2018). In the lower panel a multiplication factor of 1.5 has been applied to the HD_{DKW} modelled depth-averaged current speeds

3.3 Danish waters spectral wave model

DHI's Danish waters spectral wave model (SW_{DKW}) provides information on surface wave parameters and wave energy spectra. The model database was established through state-of-the-art numerical wave modelling software, MIKE 21 SW by DHI [10, 11]. MIKE 21 SW is a third-generation spectral wind-wave model based on unstructured meshes. The model simulates the growth, decay, and transformation of wind-waves and swell waves in offshore and coastal areas.

The wave model domain is the same as the Danish Waters hydrodynamic model described in Section 3.2 (see Figure 3.4). As for the hydrodynamic model, the spatial discretisation of wave was based on an unstructured flexible mesh with resolution of around 2 km at the Hesselø OWF (Figure 3.9). However, it should be noted that the numerical mesh of SW_{DKW} was not identical to HD_{DKW} , as the latter contained additional refinement in shallow areas and within deep-water channels that were not considered relevant for the former.

SW_{DKW} was set up with the fully spectral, in-stationary formulation, suitable for wave studies involving time-dependent wave events, and rapidly varying wind conditions (in space and time). The model was forced by 10 mMSL wind fields from the CREA6 atmospheric model (see Section 3.1). Wave conditions across the model open boundaries were provided by spatially and temporally varying wave energy spectra data from DHI's regional North Europe Hydrodynamic model (SW_{NE}). This regional wave model was also forced by CREA6 wind fields, thus ensuring consistency in the model boundary forcing (for more information on SW_{NE} please see Section 4.2 of [3]).

SW_{DKW} also includes the effects of varying water levels and current speeds that are provided from the outputs of the Danish Waters hydrodynamic model, HD_{DKW} (see Section 3.2).

Outputs from the SW_{NE} include integral wave parameters at 1-hour intervals in each model mesh element.

The performance of SW_{DKW} was evaluated at Anholt OWF, which is the closest wave validation station to the Hesselø OWF site (see location in Figure 3.9). The measurements at Anholt OWF covers approximately two months from mid-March 2010 to mid-May 2010 (see Section 2.2.4 of [4] for more information on the wave measurements). The validation results for H_{m0} at the Anholt OWF are shown in Figure 3.10. SW_{DKW} represents the measured significant wave height very, with low bias (-0.02 m) and scatter ($SI = 0.18$).

Please refer to section 3.3 of [4] for further validation of SW_{DKW} wave conditions speeds in the area around the Hesselø OWF.

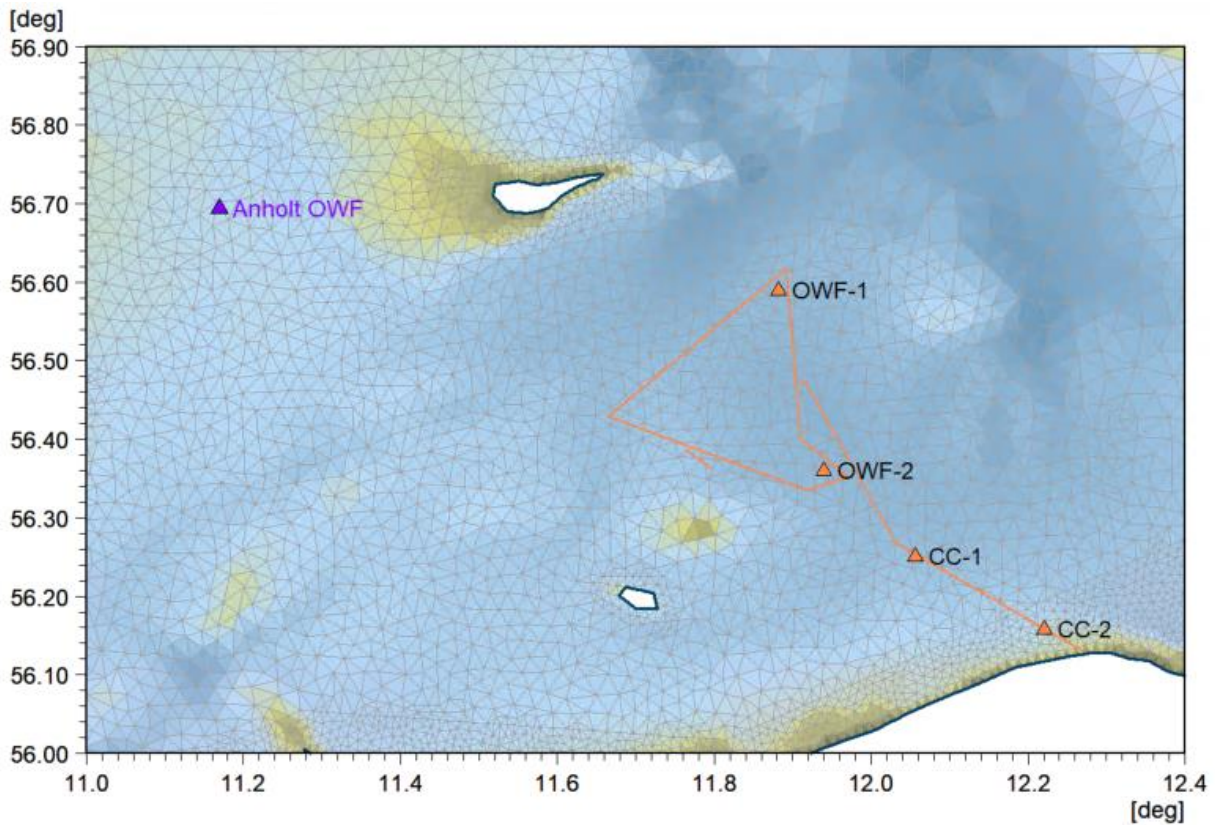


Figure 3.9 Computational mesh and bathymetry of SW_{DKW} around the Hesselø OWF
 The unstructured flexible mesh is shown by the grey triangles and the Hesselø OWF development area and export cable corridor is shown by the orange outline. The weather window analysis points (OWF-1, OWF-2, CC-1, and CC-2) are shown by the orange triangle markers. The validation station at Anholt OWF is designated by the purple triangle

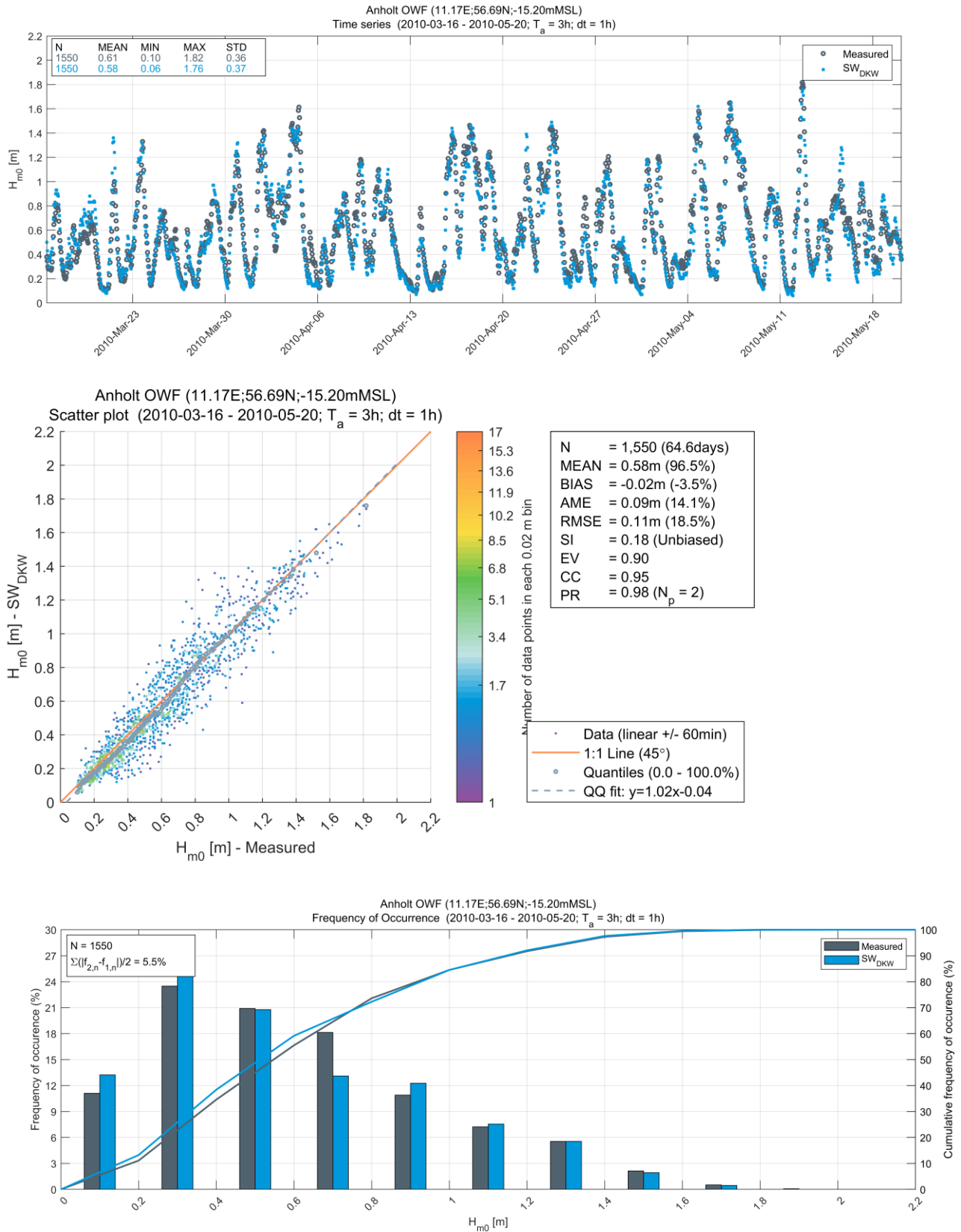


Figure 3.10 Validation of SW_{DKW} significant wave height at Anholt OWF
Time series (upper panel), scatter plot (central panel), and histogram (lower panel) comparison of modelled and measured significant wave height

4 General Metocean Conditions

A brief overview of the annual and seasonal variability of the metocean conditions at the Hesselø OWF is provided in this section.

The analysis presented in this section is based on 24-years of data (1995 to 2018, inclusive) from DHI's regional Danish Waters hindcast model database (see Section 3). Probability distribution and rose plots (based on 12 x 30° directional sectors) were used to illustrate the annual and seasonal variability in metocean conditions at the project site. The seasons were defined as follows:

- Spring: March to May (inclusive)
- Summer: June to August (inclusive)
- Fall: September to November (inclusive)
- Winter: December to February (inclusive)

Analysis point **OWF-2** was selected as a representative location of the Hesselø OWF area. The following subsections briefly describe the variability of the metocean parameter for which weather windows were assessed.

4.1 Significant Wave Height (H_{m0})

Figure 4.1 shows the annual (all-year) distribution of H_{m0} and a rose plot of the distribution of H_{m0} and mean wave direction (DWD) at analysis point OWF-2. The median H_{m0} is 0.6 m and approximately 90% of the modelled values are less than 1.5 m. The largest and most frequent waves are from the directional sectors centred at 240°N (18.9% of modelled waves) and 300°N (13.3% of modelled waves).

Figure 4.2 shows wave rose plots for each season. The largest waves occur during winter and the smallest waves during summer. During fall, winter and spring, the most frequent wave direction is from 240°N, while during summer waves from 300°N are dominant.

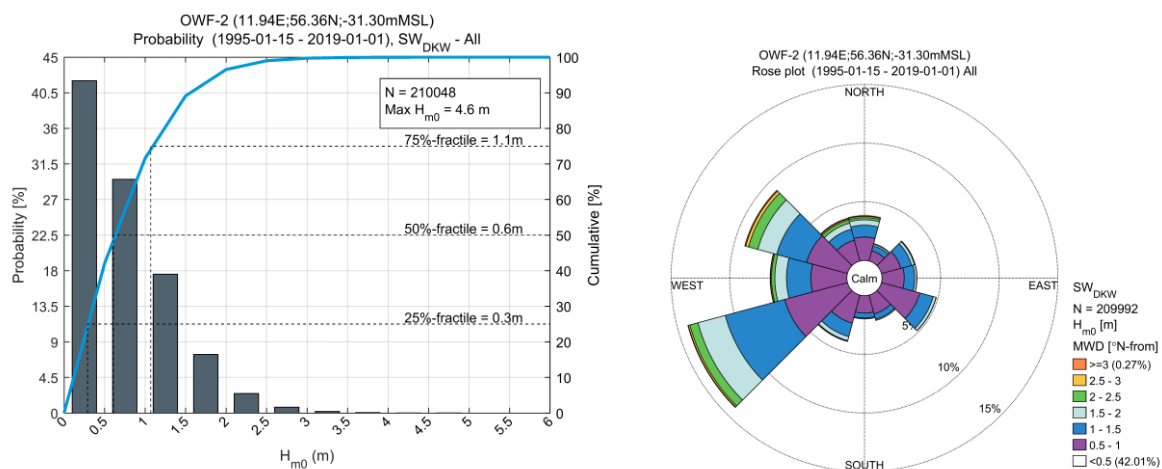


Figure 4.1 Annual variability of significant wave height at analysis point OWF-2
Left panel shows the probability distribution of H_{m0} for intervals of 0.5 m with the cumulative probability is shown by the blue line. Right panel shows the rose plot of H_{m0} against MWD

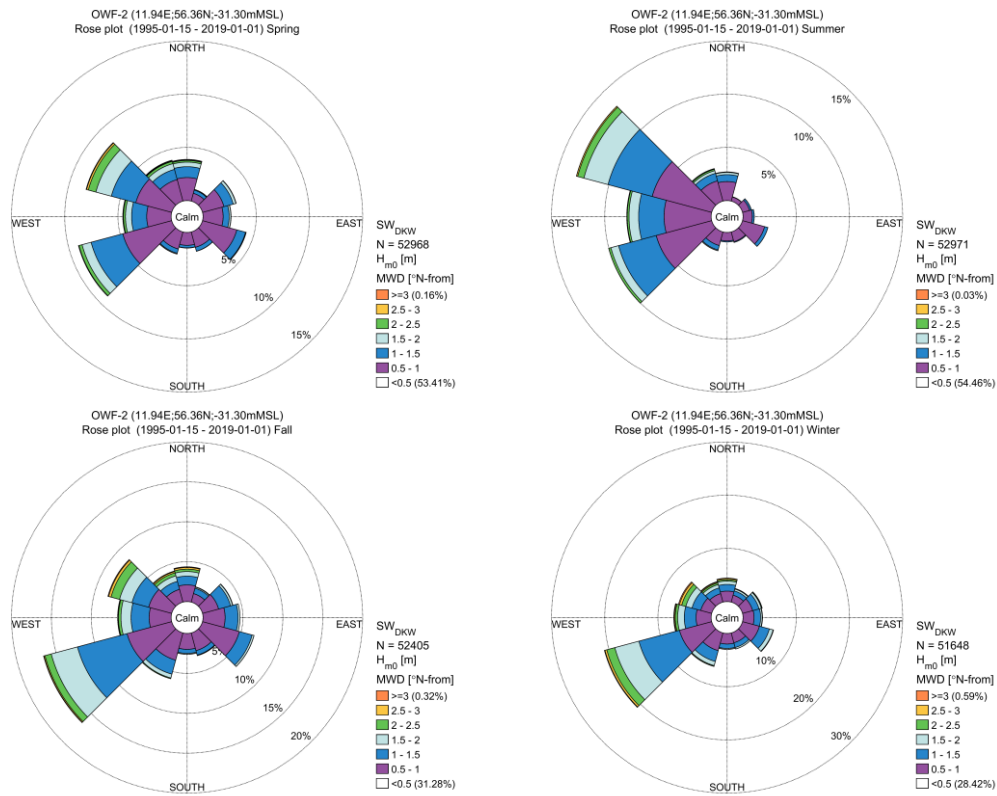


Figure 4.2 Seasonal wave rose plots at analysis point OWF-2
 Rose plots of H_{m0} against MWD for spring (upper left), summer (upper right), fall (lower left), and winter (lower right)

4.2 Current speeds

A multiplication factor of 1.5 was applied to the modelled depth-averaged current speeds (see Section 3.2). It is noted that the depth averaged current speeds do not include any effects of stratification over the water depth.

Figure 4.3 shows the annual (all-year) distribution of depth-averaged current speed (CS) and a rose plot of the distribution of CS and depth-averaged current direction (CD) at analysis point OWF-2. The median CS is 0.08 m/s and approximately 98% of the modelled CS values are less than 0.2 m/s. Currents directions are approximately bi-directional, oriented along an axis aligned 30°N to 210°N.

Figure 4.4 shows the seasonal variation in current roses at OWF-2. The mean and peak current speeds are largest during fall and winter. There is very little seasonal variation depth-averaged current direction.

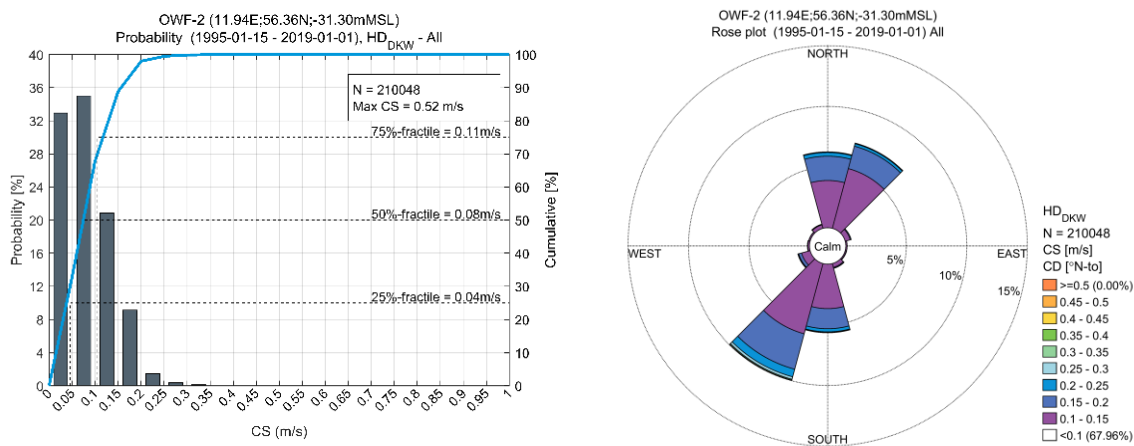


Figure 4.3 Annual variability of depth-averaged current speed at analysis point OWF-2
 Left panel shows the probability distribution of CS at intervals of 0.05 m/s with the cumulative probability is shown by the blue line. Right panel shows the rose plot of CS against CD

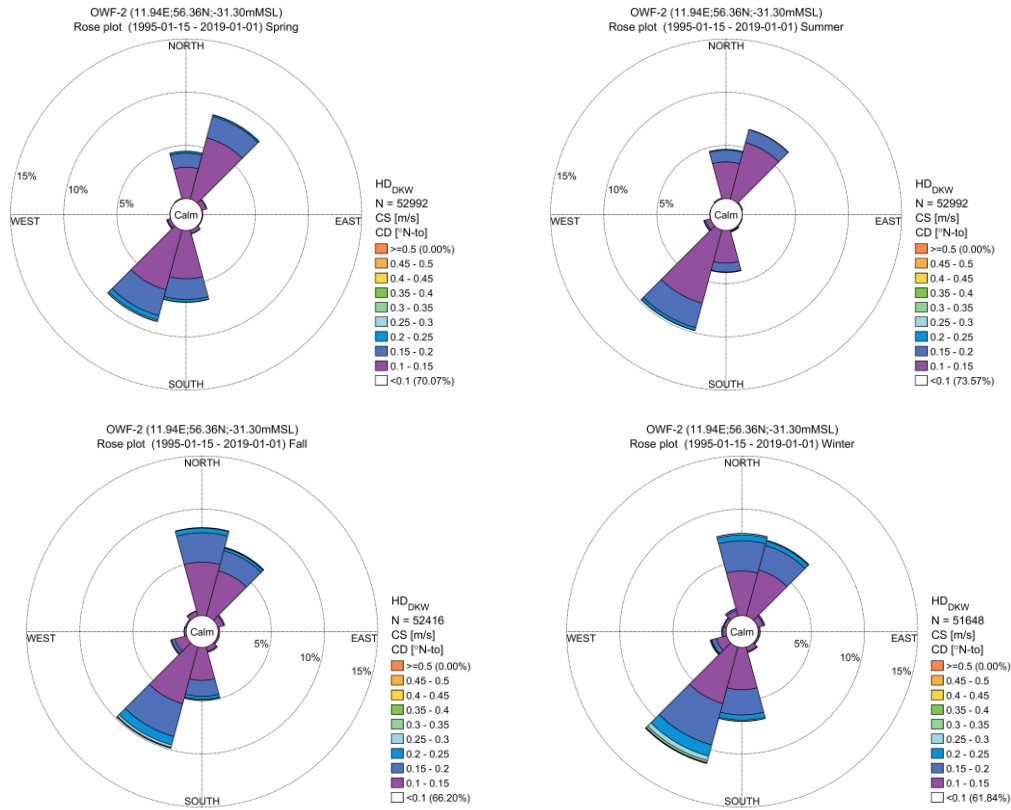


Figure 4.4 Seasonal total depth-averaged current speed roses at analysis point OWF-2
 Rose plots of distribution of CS and CD for spring (upper left), summer (upper right), fall (lower left), and winter (lower right)

4.3 Wind speeds at 10 mMSL

Figure 4.5. shows the annual (all-year) distribution of wind speed at 10 mMSL (WS_{10}) and a rose plot of the distribution of WS_{10} and wind direction at 10 mMSL (WD_{10}) at analysis point OWF-2. The median value of WS_{10} is 6.9 m/s, and 97.5% of the modelled values are lower than 15 m/s. The fastest and most frequent wind are from directional sectors centred at 240°N .

Figure 4.6 shows seasonal variation of the wind rose at OWF-2. Wind coming from directional sector centred at 240°N are most frequent during fall (12.2%), winter (16.8%), and spring (12.4%). During summer, however, winds from west (directional sector centred at 270°N) are most frequent (16.4%).

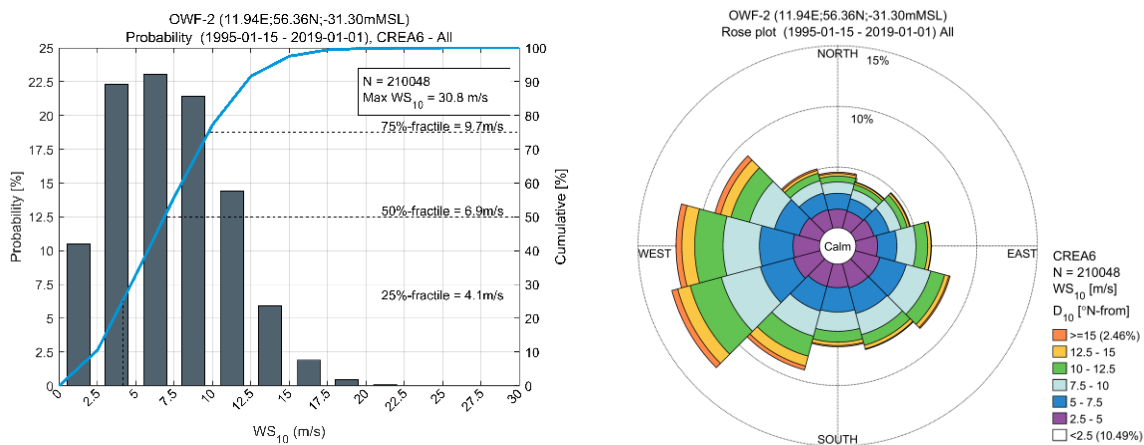


Figure 4.5 Annual variability of 10 mMSL wind speed at analysis point OWF-2

Left panel shows the probability distribution of WS_{10} at intervals of 2.5 m/s with the cumulative probability is shown by the blue line. Right panel shows the rose plot of WS_{10} against wind WD_{10}

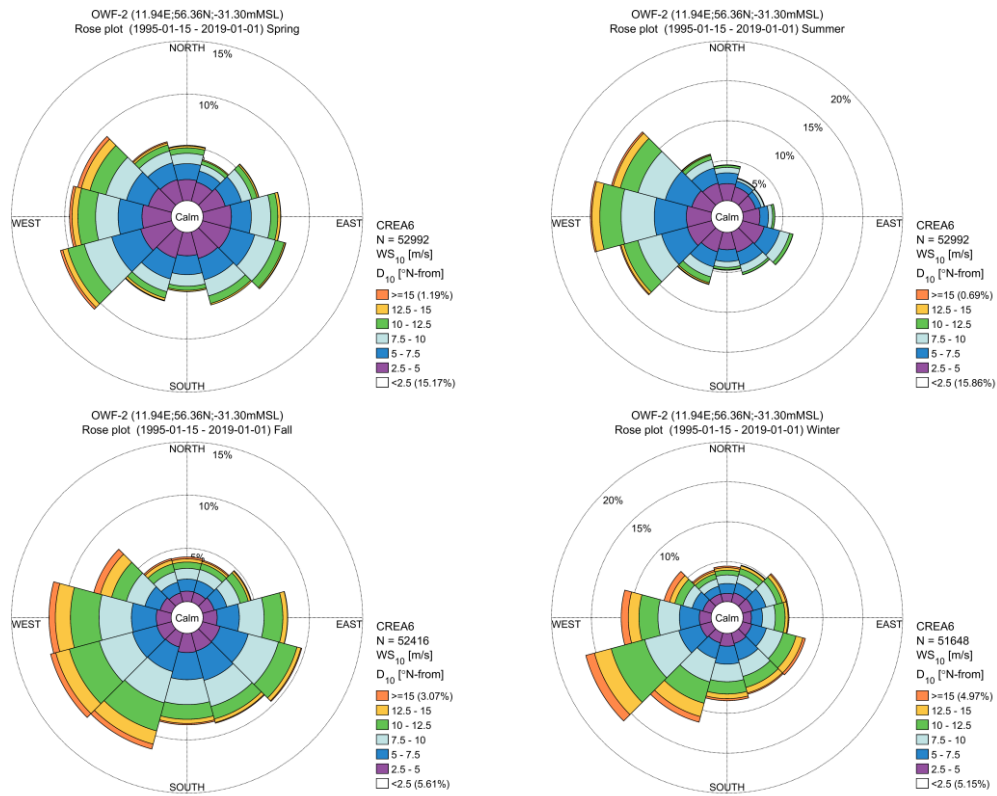


Figure 4.6 Seasonal 10 mMSL wind rose plots at analysis point OWF-2
Rose plots of distribution of WS₁₀ and WD₁₀ for spring (upper left), summer (upper right), fall (lower left), and winter (lower right)

4.4 Water levels

The total water levels at analysis point OWF-2 range from a minimum value of -0.8 mMSL to a maximum of 1.5 mMSL during the 24-year hindcast period (1995 to 2018). However, the probability distribution in Figure 4.7 reveal that 85% of the time the total water level varies between -0.3 mMSL to 0.3 mMSL.

The seasonal statistics are summarized as follows:

- Spring range between -0.8 mMSL and 1.5 mMSL with a standard deviation of 0.2 m
- Summer ranged between -0.5 mMSL and 0.9 mMSL with a standard deviation of 0.2 m
- Fall ranged between -0.6 mMSL and 1.3 mMSL with a standard deviation of 0.2 m
- Winter ranged between -0.8 mMSL and 1.5 mMSL with a standard deviation of 0.3 m.

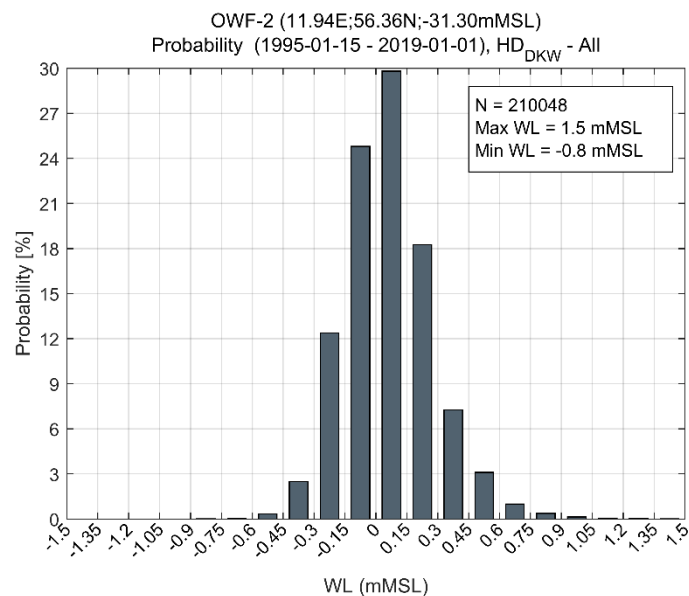


Figure 4.7 Annual (all-year) probability distribution of total water levels at analysis point OWF-2

5 Weather Window Methodology

The methodology applied to determine the operational weather windows at the Hesselø OWF is described in this section. An example of how the outputs of this analysis should be interpreted is also provided.

5.1 Description of analysis methodology

The persistence analysis, known as weather windows, is defined as a continued occurrence of a given minimum duration during which a given parameter is above/below a certain threshold. Persistence statistics of metocean parameters are applied for planning purposes of operational tasks (e.g., maintenance or construction works), and are often referred to as 'Weather Windows' and/or 'Downtime'.

A weather window is defined as a continued occurrence during which the given conditions (duration and threshold) are fulfilled, while downtime is defined as the remaining periods (i.e., all periods that are not weather windows). The sum of weather windows and downtime for any given condition will equal 100% of the time.

The durations may be defined as either 'Overlapping' or 'Non-overlapping'. An overlapping duration refers to persistence that includes the fraction of duration at the end of each weather window, while non-overlapping duration includes whole number of windows only. Overlapping duration thus results in higher occurrence of weather windows (and lower occurrence of downtime) and *vice versa*. The thresholds may be defined as being either above or below a given value depending on what is critical for the parameter in question.

Preferably, a long-term time series (several years) is applied for the calculation of persistence statistics to reduce the uncertainty related to yearly variations. The uncertainty may be estimated by calculating the persistence statistics for each available year and then deriving the mean, standard deviation and/or some given certainty percentiles. A percentile (P) above 50%, in this case, refers to a more conservative estimate, i.e., less weather windows and more downtime and *vice versa*.

In this study, the weather windows have been assessed for the following metocean parameters and thresholds:

- Significant wave height ($H_{m0} <$): 0.5 m to 5.0 m (at intervals of 0.5 m)
- Total water level (WL <): -2.0 m to +2.0 m (at intervals of 0.2 m)
- Total depth-averaged current speeds (CS <): 0.2 m/s to 1.0 m/s (at intervals of 0.2 m/s)
- Wind speed at 10 m above mean sea level ($WS_{10} <$): 5 m/s to 25 m/s (at intervals of 5 m/s)

For each parameter and threshold, the monthly statistics of weather window have been calculated for:

- Durations of 1, 6, 12, 18, 24, 30, 36, 42, 48, 54, 60, 66, and 72-hours (overlapping and non-overlapping)
- Certainty percentiles (P) of 10%, 50%, and 90%

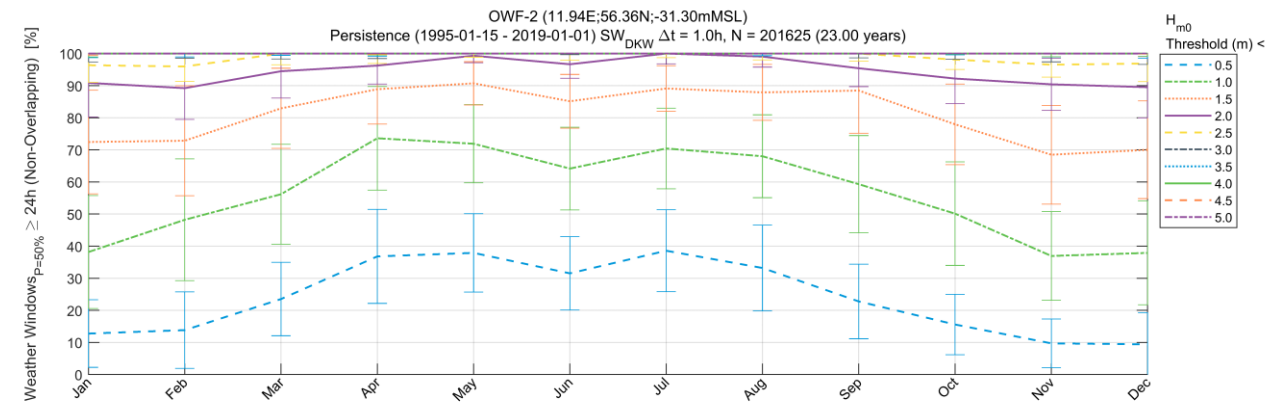
The persistence results and statistics are presented in graphical and tabular format as a percentage of time during each considered interval e.g., each calendar month. Windows stretching through more than one interval contributes with a corresponding fraction of the window to each of the intervals. Section 5.2 provides an example of the output and guidance on how to interpret the relevant statistics.

The full results for all durations, certainty percentiles, and thresholds are included as a digital appendix that accompanies this report. This includes graphical images (.jpg and .png) and tables as MS Excel files. A guide to the digital appendix is included in Section 6.

5.2 Example of weather window results

An example of significant wave height weather window analysis for a duration of 24-hours (non-overlapping) and a certainty percentile of 50% at analysis point OWF-2 is shown in Figure 5.1. The vertical bars in the plot in the upper panel of Figure 5.1 indicate \pm one standard deviation for each threshold, which are also designated by the numbers in the parentheses in the table in the lower panel of Figure 5.1. The standard deviation in these figures describes how spread the data are from the mean due to the interannual variability.

From this example, it is possible to assess that during a typical September, there is 88.5% probability of a 24-hours period during which total significant wave height is below 1.5 m. Conversely, there is a 11.5% chance that $H_{m0} \geq 1.5$ m within a 24-hour period in the same month.



OWF-2 (11.94E;56.36N;-31.30mMSL)
Persistence (1995-01-15 - 2019-01-01) $SW_{DKW} \Delta t = 1.0h, N = 201625$ (23.00 years)
Weather Windows $P=50\% \geq 24h$ (Non-Overlapping) [%]

	Jan	Feb	Mar	Apr	May	Jun	Jul	Aug	Sep	Oct	Nov	Dec
0.5	12.8 (10.5)	13.8 (11.9)	23.5 (11.4)	36.8 (14.6)	37.9 (12.2)	31.5 (11.4)	38.6 (12.8)	33.2 (13.4)	22.8 (11.6)	15.6 (9.4)	9.7 (7.6)	9.4 (9.9)
1.0	38.2 (17.6)	48.2 (19.0)	56.2 (15.6)	73.6 (16.1)	71.9 (12.2)	64.2 (12.9)	70.4 (12.6)	68.0 (12.9)	59.3 (15.1)	50.1 (16.1)	36.9 (13.8)	37.9 (16.2)
1.5	72.4 (16.1)	72.8 (17.2)	82.9 (12.5)	88.9 (10.9)	90.7 (6.7)	85.1 (8.4)	89.1 (7.1)	87.9 (8.7)	88.5 (13.3)	78.0 (12.6)	68.5 (15.4)	70.0 (15.2)
2.0	90.9 (10.6)	89.2 (9.7)	94.5 (8.4)	96.3 (5.8)	99.3 (2.2)	96.7 (4.3)	100.0 (3.2)	99.1 (3.3)	95.4 (5.7)	92.2 (7.8)	90.4 (8.1)	89.5 (9.5)
2.5	96.4 (5.4)	96.0 (4.7)	100.0 (3.5)	100.0 (3.1)	100.0 (1.1)	100.0 (2.1)	100.0 (1.3)	100.0 (2.0)	100.0 (2.3)	98.1 (3.1)	96.5 (3.9)	96.9 (5.7)
3.0	100.0 (2.6)	100.0 (1.4)	100.0 (1.7)	100.0 (1.5)	100.0 (0.0)	100.0 (0.3)	100.0 (0.0)	100.0 (0.7)	100.0 (1.3)	100.0 (1.7)	100.0 (2.6)	100.0 (3.4)
3.5	100.0 (1.3)	100.0 (1.1)	100.0 (0.6)	100.0 (0.9)	100.0 (0.0)	100.0 (0.0)	100.0 (0.0)	100.0 (0.7)	100.0 (0.0)	100.0 (0.4)	100.0 (1.0)	100.0 (1.4)
4.0	100.0 (1.1)	100.0 (0.0)	100.0 (0.0)	100.0 (0.5)	100.0 (0.0)	100.0 (0.0)	100.0 (0.0)	100.0 (0.0)	100.0 (0.0)	100.0 (0.1)	100.0 (1.0)	100.0 (0.9)
4.5	100.0 (0.5)	100.0 (0.0)	100.0 (0.0)	100.0 (0.0)	100.0 (0.0)	100.0 (0.0)	100.0 (0.0)	100.0 (0.0)	100.0 (0.0)	100.0 (0.0)	100.0 (0.0)	100.0 (0.1)
5.0	100.0 (0.0)	100.0 (0.0)	100.0 (0.0)	100.0 (0.0)	100.0 (0.0)	100.0 (0.0)	100.0 (0.0)	100.0 (0.0)	100.0 (0.0)	100.0 (0.0)	100.0 (0.0)	100.0 (0.0)

Figure 5.1 Example of weather-window analysis of H_{m0} at analysis point OWF-2
Considering a duration of at least 24-hours (non-overlapping) and $P=50\%$ with thresholds varying from 0.5 m to 5.0 m at intervals of 0.5 m. The vertical bars in the graph in the upper panel indicate the standard deviation for each threshold, which are also designated by the numbers in the parentheses in table in the lower panel

6 Deliverables (Digital Appendix)

The section provides a guide to the folder structure and filename convention of the operational weather window analysis results provided within the digital appendix.

Section 5.2 provides an illustrative example of the results of a weather window analysis of H_{m0} for a duration of 24-hours (non-overlapping) and a 50% certainty percentile. Full results for all considered parameters, thresholds, durations, and certainty percentiles are provided as digital files that accompany this document.

All persistence graphs and tables, similar to those shown in Figure 5.1, are provided as image files (.jpg and .png). The persistence statistics are also provided in a Microsoft Excel file format (.xlsx). Results are delivered in a data package within a folder named:

- 11826722_ENDK_Hesselø_WeatherWindows_DigitalAppendix

The following is intended to guide the user in navigating through the digital appendix.

There are four (4) folders in the root of abovementioned data package (see Figure 6.1). Each relates to one of the analysis points within the Hesselø OWF and export cable corridor (see Table 2.1).

Name	Date modified	Type
CC-1	13/01/2022 15:57	File folder
CC-2	13/01/2022 15:57	File folder
OWF-1	13/01/2022 15:20	File folder
OWF-2	13/01/2022 15:55	File folder

Figure 6.1 The digital appendix contains one folder per analysis point

Within each folder, there is a sub-folder relating to a different metocean parameter (Figure 6.2):

- CS: total depth-averaged current speed
- Hm0: significant wave height
- WL: total water level
- WS10: wind speed at 10mMSL

Name	Date modified	Type
CS	13/01/2022 15:30	File folder
Hm0	13/01/2022 15:33	File folder
WL	13/01/2022 15:24	File folder
WS10	13/01/2022 15:27	File folder

Figure 6.2 Digital Appendix containing one folder per metocean parameter

Each folder contains a further sub-folder referring to the definition of the duration (either *Non-Overlapping* or *Overlapping*) as shown in Figure 6.3:

Name	Date modified	Type
Non-overlapping	16-04-2021 13:45	File folder
Overlapping	16-04-2021 14:10	File folder

Figure 6.3 Digital Appendix showing the definition of duration

Herein, another set of thirteen (13) folders identify the period (durations) considered in the analysis (Figure 6.4). For instance, the folder name *DUR_24Hrs* pertains to the results associated with a duration of 24-hours.














Name	Date modified	Type
 DUR_01Hrs	12/21/2021 11:07 AM	File folder
 DUR_06Hrs	12/21/2021 11:08 AM	File folder
 DUR_12Hrs	12/21/2021 11:09 AM	File folder
 DUR_18Hrs	12/21/2021 11:10 AM	File folder
 DUR_24Hrs	12/21/2021 4:07 PM	File folder
 DUR_30Hrs	12/21/2021 11:12 AM	File folder
 DUR_36Hrs	12/21/2021 11:14 AM	File folder
 DUR_42Hrs	12/21/2021 11:15 AM	File folder
 DUR_48Hrs	12/21/2021 11:16 AM	File folder
 DUR_54Hrs	12/21/2021 11:17 AM	File folder
 DUR_60Hrs	12/21/2021 11:18 AM	File folder
 DUR_66Hrs	12/21/2021 11:19 AM	File folder
 DUR_72Hrs	12/21/2021 11:21 AM	File folder

Figure 6.4 Digital Appendix showing the thirteen (13) durations considered

Finally, within each duration folder there are a set of images files (.jpg and .png) and a single Microsoft Excel file (.xlsx) containing the weather window results (Figure 6.5).

These include the different certainty percentile values and thresholds. The image below shows the results contained within the folders:

- Analysis point OWF-2 > H_{m0} > Non-overlapping > DUR_24Hrs

The image files include plots (.jpg) and tables (.png) for the various thresholds (equivalent to those shown in the example within Figure 5.1). The file suffix indicates the analysis point name (e.g., OWF-2), and the prefix indicates the conditions (e.g., “_P=50%_Dur24h_Non-Overlapping.jpg”, is for a 50% certainty percentile, and non-overlapping duration of 24-hours).

 OWF-2_Persistence_(1995-01-15_-_2019-01-01)_Hm0_SW_{DKW}_Non-Overlapping.xls
 OWF-2_Persistence_(1995-01-15_-_2019-01-01)_Hm0_SW_{DKW}_WW_P=10%_DUR24h_Non-Overlapping.jpg
 OWF-2_Persistence_(1995-01-15_-_2019-01-01)_Hm0_SW_{DKW}_WW_P=10%_DUR24h_Non-Overlapping.png
 OWF-2_Persistence_(1995-01-15_-_2019-01-01)_Hm0_SW_{DKW}_WW_P=50%_DUR24h_Non-Overlapping.jpg
 OWF-2_Persistence_(1995-01-15_-_2019-01-01)_Hm0_SW_{DKW}_WW_P=50%_DUR24h_Non-Overlapping.png
 OWF-2_Persistence_(1995-01-15_-_2019-01-01)_Hm0_SW_{DKW}_WW_P=90%_DUR24h_Non-Overlapping.jpg
 OWF-2_Persistence_(1995-01-15_-_2019-01-01)_Hm0_SW_{DKW}_WW_P=90%_DUR24h_Non-Overlapping.png

Figure 6.5 Files containing the weather window analysis results

The accompanying Microsoft Excel files summarise the weather window statistics for the given parameter and duration combination. The file contains the results for each certainty percentile (i.e., 10%, 50%, and 90%), as identified by the sheet name. For example, the active sheet in Figure 6.6 is named *W_P=10%_DUR24h_Non-Overlapping* and relates to 10% certainty percentile.

	A	B	C	D	E	F	G	H	I	J	K	L	M
1	OWF-2 (11.94E;56.36N;-31.30mMSL)												
2	Persistence (1995-01-15 - 2019-01-01) SW_{DKW} \Deltat = 1.0h, N = 201625 (23.00 years)												
3	Weather Windows_{P=10%} \geq 24h (Non-Overlapping) [%]												
4	H_{m0}	Jan	Feb	Mar	Apr	May	Jun	Jul	Aug	Sep	Oct	Nov	Dec
5	0.5	29.3	31.4	35.4	59.4	53.7	47.9	54.9	48.1	39.9	25.3	19.4	29.7
6	1.0	66.6	67.4	76.4	89.6	86	80.8	86.7	81.5	74.2	65	62.6	59.5
7	1.5	90.4	92.8	97.1	100	100	96	98.5	98.4	96.6	87.1	95.2	87.5
8	2.0	100	100	100	100	100	100	100	100	100	98.3	100	97.2
9	2.5	100	100	100	100	100	100	100	100	100	100	100	100
10	3.0	100	100	100	100	100	100	100	100	100	100	100	100
11	3.5	100	100	100	100	100	100	100	100	100	100	100	100
12	4.0	100	100	100	100	100	100	100	100	100	100	100	100
13	4.5	100	100	100	100	100	100	100	100	100	100	100	100
14	5.0	100	100	100	100	100	100	100	100	100	100	100	100
15													
16													
17													
18													
19													
20													
21													
22													
23													
24													
25													
26													
27													
28													
29													

Figure 6.6 Example of weather wind results in Microsoft Excel format

7 References

- [1] Danish Ministry of Climate, Energy, and Utilities, “Energy Agreement,” 29 06 2018. [Online]. Available: <https://en.kefm.dk/Media/C/5/Energy%20Agreement%202018%20a-webtilg%c3%a6ngelig.pdf>. [Accessed 14 03 2022].
- [2] Danish Ministry for Climate, Energy and Utilities, “Danish Climate Agreement for Energy and Industry 2020 – Overview,” 22 06 2020. [Online]. Available: [https://en.kefm.dk/Media/C/B/faktaark-klimaaf tale%20\(English%20august%2014\).pdf](https://en.kefm.dk/Media/C/B/faktaark-klimaaf tale%20(English%20august%2014).pdf). [Accessed 14 03 2022].
- [3] DHI, “Wave and Water Level Hindcast of Danish Waters - Spectral wave and hydrodynamic modelling,” 05 2019. [Online]. Available: https://www.metocean-on-demand.com/files/share/getfile.ashx?type=document&file_name=11091004_Wave_and_Water_Level_Hindcast_of_Danish_Waters_08May2019.pdf. [Accessed 03 2022].
- [4] DHI, “Hesselø OWF, Site Metocean Conditions Assessment, Revision Final 1.0, 24 March 2022”.
- [5] C. Bollmeyer, J. D. Keller, C. Ohlwein, S. Wahl, S. Crewell, P. Friederichs, A. Hense, J. Keune, S. Kneifel, I. Pscheidt, S. Redl and S. Steinke, “Towards a high-resolution regional reanalysis for the European CORDEX domain,” *Q. J. R. Meteorol. Soc.*, vol. 141, pp. 1-15, 2015.
- [6] D. P. Dee, S. M. Uppala, A. J. Simmons, P. Berrisford, P. Poli, S. Kobayashi, U. Andrae, M. A. Balmaseda, G. Balsamo, P. Bauer, P. Bechtold, A. C. Beljaars, L. van de Berg, J. Bidlot and N. Bormann, “The ERA-Interim reanalysis: configuration and performance of the data assimilation system,” *Q. J. R. Meteorol. Soc.*, vol. 137, pp. 553-597, 2011.
- [7] DHI, “MIKE 21 & MIKE 3 Flow Model FM. Hydrodynamic and Transport Module - Scientific Documentation,” 2021. [Online]. Available: https://manuals.mikepoweredbydhi.help//2021/Coast_and_Sea/MIKE_21_Flow_FM_Scientific_Doc.pdf. [Accessed 03 2022].
- [8] D. L. Codiga, “Unified Tidal Analysis and Prediction Using the UTide Matlab Functions. Technical Report 2011-01,” Graduate School of Oceanography, University of Rhode Island, Narragansett, RI. 59pp, 2011.
- [9] R. Pawlowicz, B. Beardsley and S. Lentz, “Classical tidal harmonic analysis including error estimates in MATLAB using T-TIDE,” *Computers & Geosciences* 28, pp. 929-937, 2002.
- [10] DHI, “MIKE 21 Spectral Waves FM, Spectral Wave Module, User Guide,” 2021. [Online]. Available: https://manuals.mikepoweredbydhi.help//2021/Coast_and_Sea/MIKE21_SW.pdf. [Accessed 03 2022].

- [11] DHI, “MIKE 21, Spectral Waves Module, Scientific Documentation,” 2021. [Online]. Available: https://manuals.mikepoweredbydhi.help/2021/Coast_and_Sea/M21SW_Scientific_Doc.pdf. [Accessed 04 01 2022].

Appendix A Definition of Model Quality Indices

To obtain an objective and quantitative measure of how well the model data compared to the observed data, a number of statistical parameters so-called quality indices (QI's) are calculated.

Prior to the comparisons, the model data are synchronised to the time stamps of the observations so that both time series had equal length and overlapping time stamps. For each valid observation, measured at time t , the corresponding model value is found using linear interpolation between the model time steps before and after t . Only observed values that had model values within \pm the representative sampling or averaging period of the observations are included (e.g., for 10-min observed wind speeds measured every 10 min compared to modelled values every hour, only the observed value every hour is included in the comparison).

The comparisons of the synchronized observed and modelled data are illustrated in (some of) the following figures:

- Time series plot including general statistics
- Scatter plot including quantiles, QQ-fit and QI's (dots coloured according to the density)
- Histogram of occurrence vs. magnitude or direction
- Histogram of bias vs. magnitude
- Histogram of bias vs. direction
- Dual rose plot (overlapping roses)
- Peak event plot including joint (coinciding) individual peaks

The quality indices are described below, and their definitions are listed in Table A.1. Most of the quality indices are based on the entire dataset, and hence the quality indices should be considered averaged measures and may not be representative of the accuracy during rare conditions.

The MEAN represents the mean of modelled data, while the BIAS is the mean difference between the modelled and observed data. AME is the mean of the absolute difference, and RMSE is the root mean square of the difference. The MEAN, BIAS, AME and RMSE are given as absolute values and relative to the average of the observed data in percent in the scatter plot.

The scatter index (SI) is a non-dimensional measure of the difference calculated as the unbiased root-mean-square difference relative to the mean absolute value of the observations. In open water, an SI below 0.2 is usually considered a small difference (excellent agreement) for significant wave heights. In confined areas or during calm conditions, where mean significant wave heights are generally lower, a slightly higher SI may be acceptable (the definition of SI implies that it is negatively biased (lower) for time series with high mean values compared to time series with lower mean values (and same scatter/spreading), although it is normalised).

EV is the explained variation and measures the proportion [0 - 1] to which the model accounts for the variation (dispersion) of the observations.

The correlation coefficient (CC) is a non-dimensional measure reflecting the degree to which the variation of the first variable is reflected linearly in the variation of the second variable. A value close to 0 indicates very limited or no (linear) correlation between the two datasets, while a value close to 1 indicates a very high or perfect correlation. Typically, a CC above 0.9 is considered a high correlation (good agreement) for wave heights. It is noted that CC is 1 (or -1) for any two fully linearly correlated variables, even if they are not 1:1. However, the slope and intercept of the linear relation may be different from 1 and 0, respectively, despite CC of 1 (or -1).

The Q-Q line slope and intercept are found from a linear fit to the data quantiles in a least-squares sense. The lower and uppermost quantiles are not included on the fit. A regression line slope different from 1 may indicate a trend in the difference.

The peak ratio (PR) is the average of the N_{peak} highest model values divided by the average of the N_{peak} highest observations. The peaks are found individually for each dataset through the Peak-Over-Threshold (POT) method applying an average annual number of exceedances of 4 and an inter-event time of 36 hours. A general underestimation of the modelled peak events results in PR below 1, while an overestimation results in a PR above 1.

An example of a peak plot is shown in Figure A.1. 'X' represents the observed peaks (x-axis), while 'Y' represents the modelled peaks (y-axis), both represented by circles ('o') in the plot. The joint (coinciding) peaks, defined as any X and Y peaks within ± 36 hours of each other (i.e., less than or equal to the number of individual peaks), are represented by crosses ('x'). Hence, the joint peaks ('x') overlap with the individual peaks ('o') only if they occur at the same time exactly. Otherwise, the joint peaks ('x') represent an additional point in the plot, which may be associated with the observed and modelled individual peaks ('o') by searching in the respective X and Y-axis directions, see example in Figure A.1. It is seen that the 'X' peaks are often underneath the 1:1 line (orange), while the 'Y' peaks are often above the 1:1 line.

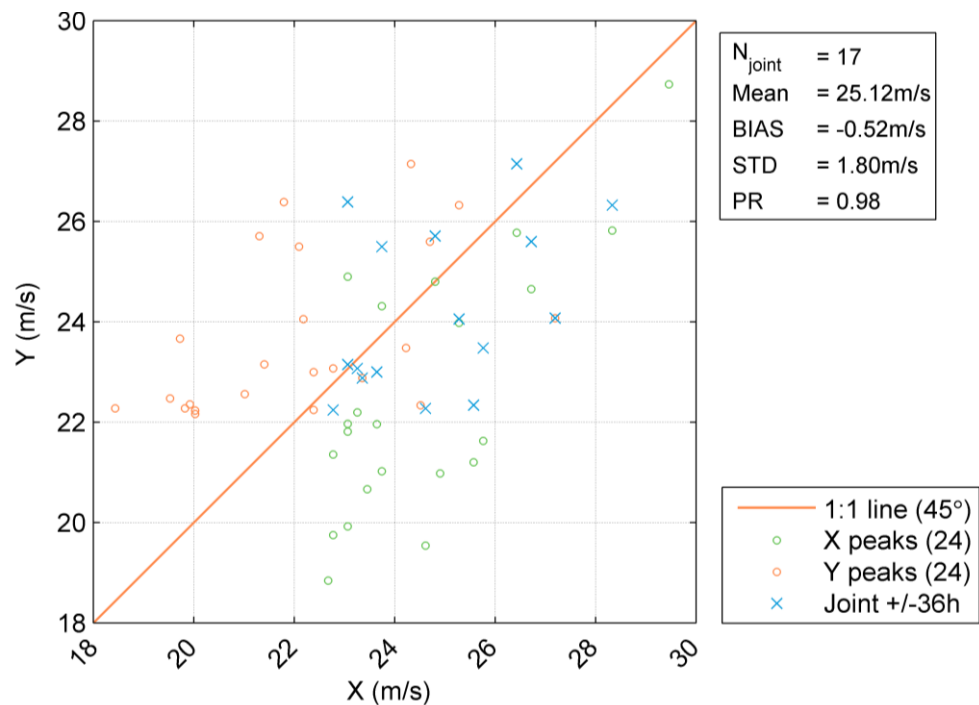


Figure A.1 Example of peak event plot (wind speed)

Table A.1 Definition of model quality indices (X = Observation, Y = Model)

Abbreviation	Description	Definition
N	Number of data (synchronized)	–
MEAN	Mean of Y data, Mean of X data	$\frac{1}{N} \sum_{i=1}^N Y_i \equiv \bar{Y}, \frac{1}{N} \sum_{i=1}^N X_i \equiv \bar{X}$
STD	Standard deviation of Y data Standard deviation of X data	$\sqrt{\frac{1}{N-1} \sum_{i=1}^N (Y - \bar{Y})^2}, \sqrt{\frac{1}{N-1} \sum_{i=1}^N (X - \bar{X})^2}$
BIAS	Mean difference	$\frac{1}{N} \sum_{i=1}^N (Y - X)_i = \bar{Y} - \bar{X}$
AME	Absolute mean difference	$\frac{1}{N} \sum_{i=1}^N (Y - X)_i $
RMSE	Root mean square error	$\sqrt{\frac{1}{N} \sum_{i=1}^N (Y - X)_i^2}$
SI	Scatter index (unbiased)	$\frac{\sqrt{\frac{1}{N} \sum_{i=1}^N (Y - X - \text{BIAS})_i^2}}{\frac{1}{N} \sum_{i=1}^N X_i }$
EV	Explained variance	$\frac{\sum_{i=1}^N (X_i - \bar{X})^2 - \sum_{i=1}^N [(X_i - \bar{X}) - (Y_i - \bar{Y})]^2}{\sum_{i=1}^N (X_i - \bar{X})^2}$
CC	Correlation coefficient	$\frac{\sum_{i=1}^N (X_i - \bar{X})(Y_i - \bar{Y})}{\sqrt{\sum_{i=1}^N (X_i - \bar{X})^2 \sum_{i=1}^N (Y_i - \bar{Y})^2}}$
QQ	Quantile-Quantile (line slope and intercept)	Linear least-squares fit to quantiles
PR	Peak ratio (of N_{peak} highest events)	$PR = \frac{\sum_{i=1}^{N_{\text{peak}}} Y_i}{\sum_{i=1}^{N_{\text{peak}}} X_i}$